Author Manuscript

Author Manuscript

Author Manuscript

Author Manuscript

HHS Public Access

Author manuscript

Nat Biotechnol. Author manuscript; available in PMC 2021 November 03.

Published in final edited form as:

Nat Biotechnol. 2021 September ; 39(9): 1078–1085. doi:10.1038/s41587-021-00897-5.

Long-term wireless streaming of neural recordings for circuit discovery and adaptive stimulation in patients with Parkinson's disease

Ro'ee Gilron[1], **Simon Little**[2], **Randy Perrone**[1], **Robert Wilt**[1], **Coralie de Hemptinne**[1], **Maria S. Yaroshinsky**[1], **Caroline A. Racine**[1], **Sarah Wang**[1], **Jill L. Ostrem**[2], **Paul S. Larson**[1], **Doris D. Wang**[1], **Nick B. Galifianakis**[2], **Ian Bledsoe**[2], **Marta San Luciano**[2], **Heather E. Dawes**[1], **Gregory A. Worrell**[3], **Vaclav Kremen**[3], **David Borton**[4], **Timothy Denison**[5], **Philip A. Starr**[1]

[1]Department of Neurological Surgery, University of California, San Francisco, San Francisco CA

[2]Department of Neurology, University of California, San Francisco, San Francisco CA

[3]Mayo Systems Electrophysiology Laboratory, Department of Neurology, Mayo Clinic, Rochester MN

[4]School of Engineering and Carney Institute, Brown University, Providence RI

[5]Department of Engineering Science, University of Oxford and MRC Brain Network Dynamics Unit

Abstract

Neural recordings in humans using invasive devices can elucidate the circuits underlying brain disorders, but have so far been limited to short recordings from externalized brain leads in a hospital setting or from implanted sensing devices that provide only intermittent, brief streaming of time series data. Here we report the use of an implantable two-way neural interface for wireless, multichannel streaming of field potentials in five patients with Parkinson's disease for up to 15

Users may view, print, copy, and download text and data-mine the content in such documents, for the purposes of academic research, subject always to the full Conditions of use: http://www.nature.com/authors/editorial_policies/license.html#terms

Corresponding author information: Correspondence and requests for materials should be addressed to R.G. roee.gilron@ucsf.edu.

Author Contributions

R.G., S.L. and P.A.S conceived the study and experiments. J.L.O., C.A.R., P.S.L, D.D.W, N.B.G., I.B. and M.S.L., provided clinical care and supervision, R.P. wrote the software interface for Summit RC+S, R.G., S.L. and R.W. collected data, R.G., S.L., S.W., C.D.H, H.E.W, G.A.W, V.K., D.B. and T.D. provided key analytic tools, R.G. and P.A.S drafted manuscript and figures.

Ethics Declaration

The study was approved by the UCSF institutional review board (IRB) under a physician sponsored investigational device exemption (IDE) from the FDA - protocol # G180097. Clinical trial is registered under: #NCT03582891 see - https://clinicaltrials.gov/ct2/show/NCT03582891. The full study protocol is available at https://osf.io/ya5jf/.

Competing interests

Devices were provided at no-charge by Medtronic inc. PAS, CDH and JLO are inventors on US patent # 9,295,838 "Methods and systems for treating neurological movement disorders"; the patent covers cortical detection of physiological biomarkers in movement disorders, which is also a topic in this manuscript.

Data Availability Statement

The data that support the findings of this study are available from the corresponding author upon reasonable request.

Code Availability Statement

Data were analyzed using Matlab 2019b (Mathworks Inc.). Code to process and analyze neural data recorded with Summit RC+S is available at https://github.com/openmind-consortium/Analysis-rcs-data and code used to create the figures in this paper is available at https://github.com/roeegilron/rcsAtHome

Author Manuscript Author Manuscript Author Manuscript Author Manuscript

months after implantation. Bilateral 4-channel motor cortex and basal ganglia field potentials streamed at home for over 2,600 hours were paired with behavioral data from wearable monitors for the neural decoding of states of inadequate or excessive movement. We validated patient-specific neurophysiological biomarkers during normal daily activities and used those patterns for adaptive deep brain stimulation. This technological approach may be widely applicable to brain disorders treatable by invasive neuromodulation.

Introduction

Electrical stimulation using permanently implanted brain devices has become a standard therapy in movement disorders and epilepsy, and is also under active investigation for psychiatric and cognitive disorders[1]. Neurostimulation therapies could be improved by a better understanding of the underlying circuit disorder and of the mechanism by which therapeutic stimulation influences signs and symptoms. One approach to addressing this knowledge gap has been the analysis of invasive cortical or subcortical field potential recordings from externalized leads, either during lead implantation surgery or for a few days afterwards in the hospital setting. Field potentials represent the summed, synchronized activity of a neuronal population near the recording contact and usually have a strong oscillatory component, thus offering an excellent probe of neural synchronization. The signs and symptoms of many brain disorders are now thought to be related in part to abnormalities of oscillatory synchronization[2].

Recordings from externalized leads provide neural data with excellent signal-to-noise ratio at high spatial and temporal resolution compared to noninvasive methods[3], but are limited by short duration, unnatural environment, and temporary circuit changes induced by edema from recent surgery. There is thus interest in incorporating a sensing function into chronic, fully implanted neurostimulators for chronic neural recording over months or years[4]. In addition to circuit discovery, an exciting potential application for these ‘bidirectional’ (sense and stimulate) neural interfaces is adaptive neurostimulation, in which stimulation therapy is automatically adjusted in response to changing brain states that are decoded from electrophysiological biomarkers of symptom severity[5, 6]. However, the early-generation bidirectional neural interfaces have important limitations[5, 7, 8]. Bandwidth and duration of data collection for time series data have been limited. Wireless data streaming typically requires patients to be ‘tethered’ to a receiving interface that restricts free movement, and requires the presence of trained investigators, constraining the use of such devices to unnatural environments. Large stimulation artifacts and amplifier saturation may preclude data collection during therapeutic stimulation.

Here we report a human study with an investigational second-generation bidirectional interface, Summit RC+S (Medtronic), which solves many of these limitations[9–11]. This device can transmit neural data at a sampling rate up to 1,000 Hz to an external Windows-based tablet up to 12 meters away, allowing freedom of movement. The interface can be tailored for easy home use and for different disease indications by programming customized functions within its application programming interface. The device’s recharging capability obviates concerns associated with prior devices that extensive sensing would

Author Manuscript Author Manuscript Author Manuscript Author Manuscript

lead to premature battery failure. This and similar devices now under development allow researchers and clinicians access to large ‘real world’ neural data sets to enable discovery of personalized neural signatures of human brain disorders.

Patients with Parkinson’s disease (PD) are an ideal population for testing novel bidirectional interfaces. PD is commonly treated with deep brain stimulation (DBS) of basal ganglia nuclei to treat motor fluctuations arising from the tendency of patients to cycle between two motor states in response to dopaminergic medications: a bradykinetic (slow) state, and a more mobile state that may be complicated by dyskinesia (excessive involuntary movement)[1]. Brief recordings have identified oscillatory activity in the basal ganglia[12] or motor cortex[13–15] as candidate neural biomarkers for specific motor signs, and have suggested that adaptive DBS might offer improved efficacy[16] or reduced adverse effects[17] compared to standard DBS. However, it is not known whether biomarkers identified in hospital settings remain useful during normal behaviors over longer periods, nor which recording site (subcortical or cortical) is most effective for motor state decoding. Further, implementing adaptive DBS at home using a fully embedded (internally controlled) algorithm remains technically challenging to implement with existing implantable devices[18–20].

To address these topics, we implanted five patients bilaterally with RC+S devices attached to both subthalamic nucleus (STN) and motor cortical leads (Figure 1). Patients streamed simultaneous multisite field potential data for several hours at home, while wearing wearable monitors for independent validation of motor state, with and without therapeutic DBS of the STN. We utilized analytic methods that leverage high volume data sets, including both supervised and unsupervised clustering methods, to test several hypotheses: that oscillatory phenomena in PD can be used to decode motor fluctuations at home during everyday activities; and that multiple recording sites improve the classification of patient motor state. We then used both subcortical and cortical oscillatory signatures of motor state as control signals, demonstrating successful adaptive DBS at home in patients with PD using a fully embedded system.

Results

Patient characteristics, surgical implant, and contact localization

Five adults received bilateral implants of the Summit RC+S bidirectional neural interface, attached to quadripolar cylindrical leads in the subthalamic nuclei, and subdural paddle-type leads over primary motor cortex (Figure 1). The paddle lead was inserted through the same skull opening as the DBS leads, which has been done safely in prior temporary[21] and permanent[8] cortical paddle placements during surgery for movement disorders. There were no surgical complications. All study subjects had idiopathic Parkinson’s disease with motor fluctuations, including prominent bradykinesia and rigidity in the off-medication states, but varied with respect to the degree of off-period tremor and on-period dyskinesia (Table 1). Data were collected up to 15 months after surgery by wireless streaming to an external computer (Figure 1). Four channels of time series recordings, two cortical and two subthalamic, were obtained from each hemisphere.

Author Manuscript Author Manuscript Author Manuscript Author Manuscript

Accurate lead placement was verified both by intraoperative physiological recordings (Figure 2 a,b) and anatomically by postoperative CT scan computationally fused with preoperative MRI scan (example lead locations Figure 2c; lead locations for all patients are provided in Table S1 and Extended Data Figure 1). Therapeutic continuous STN neurostimulation (standard clinical therapy) was initiated at one month post-implantation. There were no serious adverse events related to surgery or to the study protocol. Including all study subjects, a total of 2655 hours of 8 channel recordings were collected. Recording durations for each subject are in Extended Data Figure 2. Brief in-clinic recordings were obtained to verify the presence of movement related activity, and the effects of levodopa in defined on/off states (Extended Data Figure 3, further details in supplemental results)

Physiological signatures of motor signs identified by pairing at-home neural recordings with wearable monitors

At 2–4 weeks after device implantation, prior to initiating standard clinical neurostimulation, patients streamed eight-channel neural data at home over a total of 2142 hours. Data were collected while patients were on their usual schedule of antiparkinsonian medications, during normal activities of daily living, in both awake and asleep states. Patients wore clinically validated wrist-mounted wearable monitors bilaterally (Parkinson's KinetiGraph (PKG) watch)[22]. These provided numerical scores for bradykinesia and dyskinesia every 2 minutes based on a 10-minute moving average (Figure 3). Neural data were also analyzed in 10 minute segments, to correspond to the length of time over which behavioral data were segmented. Superimposed 10-minute power and coherence spectra for all recordings paired with behavioral data are provided in Extended Data Figure 4. For awake data, these 10 minute data segments were segregated into mobile ("estimated on") and immobile (estimated "off") segments by PKG scores and their power spectra and coherence were averaged.

All patients experienced motor fluctuations as evident from their PKG watch data with periodic variations in scores (example in Figure 3a). A time-frequency analysis over a single day from a single subject with severe motor fluctuations shows that transitions between on and off states were associated with simultaneous rapid transitions in beta and gamma band oscillatory activity, as well as in in coherence between STN and cortex (Figure 3b). Averaged power spectra segregated by the wearable monitor (42.7 hours of recording) showed a prominent STN beta band peak when in the off state, which disappeared in the on state, and a prominent motor cortex gamma band peak at 75 Hz when on with dyskinesia (Figure 3c). STN-motor cortex coherence changes in these frequencies are also evident. Segregating neural data according to behavioral states defined by wearables is a form of supervised clustering. When objective behavioral data are not available, unsupervised clustering methods may also reveal distinct brain states (Extended Data Figure 5, further details in supplemental results)

We systematically evaluated individualized neural biomarkers, by calculating p-values for significant differences between mobile and immobile states in canonical frequency bands (Figure 4). This revealed a subject-specific "fingerprint" of neural signatures. In many subjects, STN-motor cortex coherence in beta or gamma bands prominently distinguishes

Author Manuscript Author Manuscript Author Manuscript Author Manuscript

mobile and immobile states, underscoring the potential for use of inter-region oscillatory interactions for the evaluation of motor function. When present, alpha band coherence peaks at 10 Hz were typically distinct from that subject's beta band coherence, and may represent a tremor-related phenomenon at "twice tremor frequency"[23]. Of note, patients with high off-period tremor scores (Table 1) may have less prominent differences in STN beta activity in mobile versus immobile states, consistent with the known suppressive effect of off-period tremor on STN beta oscillations[24]. Recording during sleep (1502 hours total) showed that sleep suppresses subthalamic beta band and cortical gamma band oscillations, as well STN-cortex coherence in both bands (Examples in Extended Data Figure 6).

Recording sites and disease profiles for optimal motor state decoding

The specificity and sensitivity of oscillatory phenomena for decoding motor states was quantified by building a *within-subjects* linear model that utilized neural data to predict mobile and immobile states (as defined by the PKG wearable monitor). The model was trained using 5-fold stratified cross validation. The significance of decoding was then tested within-subjects non-parametrically by shuffling the "on" and "off" labels and repeating the 5-fold cross validation. Spectral power in beta or gamma bands, computed from 10-minute single channel recordings within a target (STN or motor cortex) was predictive of motor state in most but not all hemispheres (Figure 5a, black boxes). Decoding improved when combining both spectral features and both recording channels within a target (Figure 5a, grey boxes), and improved further when both recording sites were combined and cortex-STN coherence was included (AUC range 0.81–1.0, Figure 5a grey solid box). Of note, one subject, RCS01, had high AUC values even for single site recording and overall the highest AUC. This subject had the most severe fluctuations in rigidity and akinesia. Across subjects, severity of fluctuations had a trend toward correlation with the accuracy of decoding (Figure 5b). These results underscore the utility of *multisite* sensing for biomarker identification for subjects with milder fluctuations in motor signs.

Adaptive DBS at home

Most PD patients on standard open loop DBS continue to require dopaminergic medications for optimal function, but these can continue to result in motor fluctuations between mobile and immobile states. The mental model underlying our adaptive algorithm was to utilize a neural signature of medication-induced motor fluctuations and utilize that signature to adjust stimulation amplitudes over a slow time scale (minutes-hours). We utilized two different control strategies in two subjects, one based on STN beta band oscillations (Figure 6a) and one based on cortical gamma band activity (Figure 6b). These were designed to deliver increased stimulation selectively while the patient was in an immobile, "off" period (Figure 6a), or to deliver decreased stimulation selectively when the patient was in a dyskinetic state (Figure 6b), so as improve bradykinesia control while avoiding the stimulation-induced dyskinesias that tend to occur in "on" periods.

In both cases, stimulation amplitude adjusted appropriately to changes in neural biomarkers over multiple cycles of motor fluctuations. For RCS01, objective data from the PKG monitor as well as subjective data from motor diaries, during a home trial spanning four consecutive days (daytime only), showed increased "on" time without dyskinesia during adaptive DBS

Author Manuscript Author Manuscript Author Manuscript Author Manuscript

compared to clinically optimized open loop DBS (Figure 6d) and Supplemental video. Further details on sensing during stimulation are provided in Extended Data Figure 7 and in supplemental information).

Discussion

Here we report human use of an implanted bidirectional neural interface designed for continuous wireless streaming of neural data for long periods, at home during normal daily activities. We use this to show in five PD patients, implanted bilaterally with both motor cortex and basal ganglia leads, that patterns of oscillatory activity in both structures can decode states of mobility and immobility, as demonstrated by pairing the recordings with wearable monitors that track these motor fluctuations behaviorally. We implemented embedded adaptive DBS at home over four consecutive days utilizing either subcortical or cortical signals, to adjust stimulation levels based on neural detection of motor fluctuations and found clinical benefit compared to standard open loop DBS. To our knowledge, no previous study has demonstrated adaptive DBS in PD at home during normal activities.

Most prior studies of oscillatory neural signatures of specific motor signs in PD have been performed over brief periods (minutes) using externalized brain leads. High-volume chronic streaming of invasive recordings at home produced several findings not readily achievable with brief recordings. First, we identified biomarkers relevant to patients' function in their real world environments. For example, prior work has pointed to subthalamic beta band oscillations as an index of severity of the rigid/akinetic state, and as a measure of response to therapy[12], but those studies were done in the absence of voluntary movement, and in the context of artificially extreme, investigator-induced medication states. Here, we provide validation that subthalamic beta activity and other neural signatures provide real-world biomarkers of motor fluctuations, as experienced by patients without constraints on movement and behavior, and on their habitual medication schedules. Second, we identified individual variations in neural signatures of motor state, which are expected because PD patients vary in their specific motor signs. Previous brief in-clinic studies required statistical comparison *across* a group of subjects, which identifies common biomarkers but obscures individual variations. Here, the analysis of high-volume longitudinal data offered the statistical advantage of *within-subjects* comparisons of neural activity over many exacerbations and remissions of specific signs and symptoms of disease states, providing patient-specific "fingerprints" of neural activity (Figure 4). Third, chronic at-home recordings demonstrate the profound effect of sleep on neural biomarkers of motor state (Extended Data Figure 6), which is impractical to obtain from brief in-clinic recordings. All three of these elements are critical for the use of these putative biomarkers as control signals for adaptive DBS.

While continuous, constant-amplitude neurostimulation is now employed in many conditions, it may induce adverse effects such as hypophonia[17] or dyskinesia[13] in PD, mania in OCD[25], or seizures from cingulate stimulation for pain[26]. The efficacy of continuous stimulation may also suffer from waning effectiveness, such as in chronic pain[27] or essential tremor[28]. If stimulation were adjusted contingent on the relevant patterns of abnormal circuit activity, it could respond to changing brain needs and reduce adverse effects[6, 29]. Here, we

Author Manuscript Author Manuscript Author Manuscript Author Manuscript

provide a demonstration of adaptive DBS in PD at home (Figure 6), using an implanted device in a totally embedded configuration (no external links), using either basal ganglia or cortical control. For implementation of adaptive DBS, sensing from the same contact array as used for therapeutic stimulation is attractive in that it obviates the need for additional brain leads. It has been technically challenging, especially for subcortical structures, due to the low amplitude of the relevant signals (<10 μV) in comparison with stimulation artifact. Previous bidirectional interfaces have usually only allowed meaningful sensing in the absence of stimulation or by sensing from a distant contact array[19].

While subjects showed evidence of therapeutic benefit from adaptive DBS, we did not perform a formal clinical trial of adaptive DBS. Much work remains to design a rational approach to selecting the control strategy and to optimizing parameters within each strategy. Control strategies may work on fast time scales such as those designed to reshape bursts of oscillatory activity over hundreds of milliseconds[30], or on slower times scales in which neural signals are used to track motor fluctuations over minutes to hours, as demonstrated here.

Our results also point to potential advantages of *multisite* sensing. The *combination* of cortical and basal ganglia signals provided improved motor state decoding in patients with less profound motor fluctuations (Figure 5). Adaptive DBS algorithms that incorporate both sites might provide the most precise adaptive control for those cases. Multisite recordings also revealed a potentially rich biomarker space in inter-region coherence. This has also been shown to be the case in decoding mood from neural signals[31], suggesting that coherent activity between distant sites could prove useful in adaptive DBS for psychiatric states as well as for PD.

Unidirectional DBS devices (stimulation only without sensing) have been commercially available for thirty years and surgical morbidity for their placement is low[1]. Several fully implantable brain devices that combine neural sensing with therapeutic neurostimulation have been introduced prior to the present work. The RNS device (NeuroPace) has been used for contingent stimulation in some types of epilepsy[5] and in Tourette's syndrome[32]. A first-generation precursor of RC+S, Activa PC+S (Medtronic), has been used under investigational protocols for brain sensing in PD[8, 13, 33–36], essential tremor[20], epilepsy[37], pain[26], and locked-in syndrome[38]. However, both devices are designed for brief recording rather than continuous streaming of time series data, are problematic for recording during therapeutic stimulation on adjacent contacts of an array[33], and are inflexible with respect to the type of adaptive DBS algorithms that can be embedded[4]. In the second-generation RC+S, device features conducive to sensing during stimulation include signal blanking during stimulation for variable intervals, and "active recharge" mode, which reduces the duration of the second phase of each biphasic square wave stimulus, compared to passive recharge mode. A recently introduced commercial sensing device, the Percept (Medtronic) allows long term streaming of spectral power in a predefined frequency band[39]. However, this more restrictive form of long term data streaming, unlike streaming of time series data, requires *a priori* knowledge of the most relevant frequency band, and does not allow evaluation of broadband responses nor exploration of many other metrics of neuronal synchronization[13, 40, 41].

Author Manuscript Author Manuscript Author Manuscript Author Manuscript

A new challenge of RC+S, inseparable from its high flexibility, is the requirement for academic investigators to write their own software to control its functions, and to document its compliance with FDA requirements. Investigators thus need to hire or contract with a dedicated software engineer familiar with medical devices, or collaborate closely with other groups that do so. Here, this complexity was mitigated by establishing a multi-institutional collaborative environment in which device control software and regulatory templates (including the investigational device exemption for this study) are freely shared between academic groups (https://openmind-consortium.github.io).

Devices for chronic wireless invasive neural recording during normal behavior at home are now available. We show how this technology is advantageous for signal discovery compared with brief in-clinic recordings, and provide a successful demonstration of embedded adaptive DBS in PD at home. Similar approaches may be widely applicable to neurologic[6] and psychiatric[29] disorders.

Methods

Inclusion criteria and clinical characterization.

The study was approved by the hospital institutional review board (IRB) under a physician sponsored investigational device exemption (IDE), protocol # G180097, and was registered at ClinicalTrials.gov (NCT03582891). Patients provided written consent in accordance with the IRB and the Declaration of Helsinki. Five study subjects were recruited from a population referred for implantation of deep brain stimulators for PD. Subjects were evaluated by a movement disorders neurologist and met diagnostic criteria for PD[1]. Baseline motor function was evaluated using the Movement Disorders Society (MDS) Unified Parkinson's Disease Rating Scale (UPDRS), parts I-IV. The motor subscale (UPDRS-III), was rated both "off" (12 hour after withdrawal of antiparkinsonian medication) and "on" (after a supratherapeutic dose of levodopa/carbidopa). Patients were evaluated by a neuropsychologist to exclude significant cognitive impairment or untreated mood disorder. Inclusion criteria were: Motor fluctuations with prominent rigidity and bradykinesia in the off-medication state, baseline off-medication MDS-UPDRS-III scores between 20 and 80, greater than 30% improvement in MDS-UPDRS-III on medication compared to off medication, and absence of significant cognitive impairment (score of 20 or above on the Montreal Cognitive Assessment). The full IDE application (# G180097) and study protocol have been shared with other researchers via the Open Mind initiative (https://openmind-consortium.github.io).

Surgery, device models, and lead localization.

All patients underwent bilateral placement of cylindrical quadripolar deep brain stimulator leads into the subthalamic nucleus (Medtronic model 3389, 1.5 mm contact length and 2.0 mm intercontact spacing), bilateral placement of paddle-type quadripolar cortical paddles into the subdural space over motor cortex (Medtronic model 0913025, 4 mm contact diameter and 10 mm intercontact spacing), and bilateral placement of investigational sensing implantable pulse generators (IPGs) in a pocket over the pectoralis muscle (Medtronic Summit RC+S model B35300R). The IPG and leads were connected by 60 cm lead

Author Manuscript Author Manuscript Author Manuscript Author Manuscript

extenders (Medtronic model 37087), two on each side (Figure 1). STN leads were initialized as contacts 0 to 3 (0 is the deepest contact, Figure 2a). Cortical leads were initialized as contacts 8 to 11 (8 is the most posterior contact, Figure 2c).

The surgical technique for placement of permanent subdural paddle leads during DBS implantation surgery was previously described in detail[2]. Further surgical details are provided in Supplemental Information.

Two months postoperatively, locations of leads were again verified, by postoperative CT computationally merged to the patient's preoperative MRI using Stealth8 Cranial software (Figure 2c and Supplementary Figure 1).

RC+S device characteristics and programming.

The Summit RC+S is an investigational rechargeable bidirectional neural interface that offers the researcher a great degree of flexibility through access to the device's application programming interface (API)[3, 4]. It is a 16-channel device that can simultaneously stream four bipolar time domain channels (250/500 Hz) or two channels at 1000 Hz. It can simultaneously provide standard therapeutic stimulation on up to two quadripolar leads, and can also perform adaptive deep brain stimulation using algorithms programmed on the device ("embedded" mode) or algorithms on an external computer, through wireless communication ("distributed" mode). In addition to voltage time series data, RC+S can stream up to 8 predefined "power channels" (spectral power within a predefined frequency band), and data on the subject's movement from an embedded accelerometer.

For all research functions including configuring and initiating sensing, and developing embedded or distributed adaptive DBS, investigators controlled the device by writing software in C# within the device API, accessed using a "research development kit" (RDK, Medtronic model 4NR013) provided by the manufacturer. We wrote two graphical user interface (GUI)-based applications to configure and initiate streaming data from one or two RC+S devices simultaneously. One application was used by the research team and allows configuration of sensing parameters and streaming data in-clinic. The other application was "patient facing" and contains a simplified application that allows the patient to control streaming in a home environment and report symptoms or medications taken. Applications rely on a dynamic linked library (DLL), supplied by Medtronic, Inc., that is specific for Microsoft Windows operating systems and Intel processor platform. The DLL provides the API to investigators and is not compatible with streaming data to mobile devices. Both applications are available at https://openmind-consortium.github.io. We wrote and documented software in compliance with FDA code of federal regulation CFR 820.30, which specifies design controls for implantable human devices. Figure 1 provides a schematic of the data streaming configuration.

In-clinic data recording in defined on/off states.

STN and cortical field potentials were sampled at 500 Hz in clinic three weeks postoperatively in both "on" and "off states (during which levodopa medication was withdrawn for at least 12 hr), and a movement disorders neurologist administered the MDS-UPDRS-III rating scale in both states. The three week time point was chosen to

Author Manuscript Author Manuscript Author Manuscript Author Manuscript

allow recovery from the "microlesion" effect of lead insertion[5, 6], but prior to initiating chronic therapeutic stimulation at 1 month after surgery. Recordings were done at rest, and during a touch-screen based center-out reaching task similar to one previously described[7]. Rest recordings were 1–2 minutes long, and reaching task recordings were 3–5 minutes long. Details of the statistical analysis of in-clinic recordings are provided in Supplemental Information.

At home data streaming paired with wearable monitors.

Patients initiated home recordings using the patient-facing GUI on a Microsoft Surface Go computer with broadband cellular service (weight 1.15 pounds, dimensions 245.00 × 175.00 × 8.30 mm (height, width, thickness)). A lightweight telemetry bridge (191.07 grams, 154 × 61 × 22 mm (height, width, thickness)) is carried by the patients on their person and transmits data received from the IPG in the MICS-band (Medical Implant Communication Service) short range radio to an encrypted Bluetooth signal. The Bluetooth signal is received by a laptop computer provided to each study subject along with training in its use (Figure 1). Streamed data contained no personal health information (PHI). Data were encrypted and uploaded to a secure cloud environment operated by UCSF. Patients were able to use the application to report medications taken and to rate their motor signs. The application automatically connects to the device when patients are in range (approximately 12 meters). Patients collected data in 1–2 week recording "sprints" in which they were instructed to carry the computer with them and stream continuously if possible.

The summit RC+S system uses a user datagram protocol (UDP). Data are transmitted in discrete intervals or "packets" of variable duration averaging 50 ms. Occasional data packets are lost and these "dropped packets" must either be interpolated or discarded. This can also be partially mitigated by changing sampling rates and using a lower data streaming bitrate. Failure of packet transmission ("dropped packets") occurred for 1–5% of packets, even when patients were in range of receiving devices. We have written specialized software in Matlab to account for dropped packets which is available on our GitHub page https://github.com/openmind-consortium/Analysis-rcs-data.

Data are time stamped using the pulse generator clock time. Most data were recorded at 250 Hz. During an at-home computer controlled movement task (described below) data were streamed at 1000 Hz. During patients' activities of daily living, four time domain channels were streamed using a bipolar recording configuration in which we verified adequate signal during a montage recording obtained one to two days postoperatively. Patients also streamed actigraphy at 64 Hz from the embedded accelerometer, and power channels. The Summit RC+S device has several configurable device filters[3, 4] that must be chosen. All filters are applied after digitization, and low pass filters are applied twice – before and after amplification. In the absence of therapeutic stimulation, we used a high pass filter of 0.85 Hz and low pass filter of 450 Hz before amplification and 1700 Hz after amplification.

To track parkinsonian motor signs at home, for subsequent correlation with paired neural data, patients wore wristwatch style monitors (Parkinsons's KinetiGraph System (PKG), Global Kinetics Inc)[8, 9]. The PKG reports scores for bradykinesia, dyskinesia and tremor every two minutes as well as the timing in which medication were taken. The PKG uses a

Author Manuscript Author Manuscript Author Manuscript Author Manuscript

3 axis accelerometer (similar to that embedded in RC+S) to assess parkinsonian symptoms according to a proprietary commercial algorithm that has been validated[10]. We confirmed accurate temporal synchronization between the PKG and the RC+S by comparing their actigraphy data. Further details on maintaining continuity of data streaming are provided in Supplemental Information.

Therapeutic continuous stimulation and recording during stimulation.

To implement standard DBS therapy, clinicians were provided a tablet programmer (Medtronic model 4NR010) to set parameters for standard continuous therapeutic stimulation, and a patient programmer (Medtronic model 4NR009) that allows the patient limited control over some parameters under limits set by the clinician. One month after implantation, study clinicians began programming the STN (subthalamic nucleus) leads for optimum clinical benefit. The cortical lead was never used for stimulation. Clinicians attempted programming using monopolar mode from one of the middle two contacts (contacts 1 or 2), as these montages are compatible with bipolar sensing in a "sandwiched configuration" around the stimulating contact. Sensing from STN leads programmed to stimulate in a bipolar mode or programmed with a stimulation montage that includes contacts 0 or 3, precludes STN sensing during stimulation because of excessive stimulation artifact. Data were also streamed at home during therapeutic stimulation, to document effects of stimulation on STN and cortical field potentials. Both on-device low pass filters were set at 100 Hz for STN recordings during stimulation to limit stimulation artifacts). Sense blanking (used to mitigate stimulation artifact) was set at 0.33 ms.

Data extraction and management of lost data.

Data streamed to the researcher or patient facing applications are assembled into JavaScript Object Notation (.JSON) format. This is a light-weight data-interchange text-based format that in RC+S merges meta-data and actual data across several different file types. Data are streamed from the device in configurable intervals (50 ms in our case) in first-in, first-out (FIFO) fashion. The IPG has a 16 bit clock-driven tick counter that rolls over every 6.553 s (least significant bit (LSB 100 μs)). This can be combined with an estimate of system time (LSB seconds) to accurately account for lost packets. We wrote Custom software in Matlab to extract the data from the .JSON format and discard packets that have corrupted data. The extraction code and details about accurate accounting for lost packets is available on GitHub (https://github.com/openmind-consortium/Analysis-rcs-data).

Neural data collection and processing for home data during activities of daily living.

Data were divided into 30 s contiguous chunks in which no packet loss occurred. We calculated the PSD using the Welch Method in Matlab (pwelch, 250 ms window, 125 ms overlap). Data were averaged in the power domain between 40–60 Hz (range selected to avoid frequency bands of physiological interest) and outliers larger than 2 standard deviations were excluded from further analysis. This was usually due to the presence of transient artifacts in the data and only affected 1.3% on average (range 0.1–3.1%) of the data. For some analyses, data were normalized by dividing each PSD by the average power between 3 and 90 Hz (Figures 4,5,7,8, S2) to better account for impedance and stimulation effects over time. In addition to the PSD, the magnitude squared coherence was

Author Manuscript Author Manuscript Author Manuscript Author Manuscript

also computed for the four possible contact pairs in each recording montage (mscohere in Matlab, 256 ms window, 50% overlap, 256 discrete Fourier transform points). Further details on collection of task related data are provided in Supplemental Information.

Use of wearable PKG monitor to categorize motor state during activities of daily living

The PKG monitor produced a numerical score for severity of specific motor signs, in time increments of 2 minutes. Only scores for bradykinesia and dyskinesia were used in the behavioral categorization of mobile and immobile states. Bradykinesia scores are negative such that a lower score (a negative number of greater magnitude) indicates more bradykinesia. Dyskinesia scores are positive such that a higher score indicated more dyskinesia. In general, a patient was scored as immobile ("off") for each 10 min segment, if their bradykinesia scores were lower than −26 (farther from zero) but greater than −80, and dyskinesia scores below 7. A patient was scored as mobile ("on") if the bradykinesia score was higher than −26 (closer to zero) or if the dyskinesia score was above 7. Sleep was defined as a bradykinesia score below −80. These thresholds were based on the manufacturer's recommended thresholds for moderate or severe motor signs.

Using these guides, patient "on" vs "off" state were tailored on an individual basis given each patient's clinical condition. For example, some patients never had on-time without dyskinesia whereas others did not have any dyskinesia as measured by the PKG. Even though severity scores were updated every 2 min, states were defined using a 10 min window based on manufacturer recommendations. A patient was deemed in a specific "state" if at least 60% of 2-min epochs within a 10 min window were in agreement with regards to patient state. If this criteria is not met, state was classified as "other" (Figure 5a). For each 10 min window of PKG data, the corresponding 30 s PSD's from the RC+S on the contralateral side were averaged. The use of 30 s PSDs was to avoid transients in the 10 min windows resulting from small gaps in the data.

While dyskinesia scores were used in combination with bradykinesia scores for behavioral segregation of immobile and mobile states, we did not generally subdivide mobile states into those *with and without* dyskinesia, with the exception of adaptive DBS testing in one subject with severe dyskinesias, RCS01 (Figure 6d). Of note, while sleep was categorize by PKG monitor for all analyses that relate behavioral data to neural data (Figures 3–5 as well as Supplemental Figure 1 and Extended Data Figure 6), some analyses used larger sets of data that included intervals during which the PKG was not worn. In those analyses, sleep was defined temporally as between 10 pm-8 am for large data pools that included segments for which the PKG was not worn (Extended Data Figures 2,4,7).

Synchronization of neural data with wearable monitor state estimates.

Since the RC+S device streams data to a laptop computer it has a measurement of the computer clock on a per packet (~50ms of data) basis. The computer clock time was used to synchronize neural data with the PKG data (which provides a score every 2-minutes). The RMS voltage of the internal built-in accelerometer was used in order to verify the synchronization between the PKG and the RC+S data.

Author Manuscript Author Manuscript Author Manuscript Author Manuscript

Identification of frequency bands that predict immobile and mobile states, within subjects.

To assess the statistical significance of biomarkers that distinguished mobile and immobile states in specific frequency bands in home recordings, we analyzed each subject *individually*. For each subject, contact and measure (coherence/ spectral power) we defined a 4 Hz window around oscillations in three a-priori defined frequency bands: alpha (8–12 Hz), beta (12–30 Hz) and gamma (50–90 Hz). Oscillatory activity was defined as present, where there was a spectral peak in the specified pre-defined frequency range using Maltab findpeaks algorithm. We then computed a ranksum test between PKG defined "on" and "off" state estimate from all PSD's and corrected the results for multiple comparisons within each subject (Figure 4).

Linear discriminant modelling.

In addition to determining which frequency bands distinguished mobile and immobile states in each subject (Figures 3 and 4), we also sought to determine whether combinations of neural features were more sensitive and specific for predicting motor state, than individual features. To do this, we trained two "types" of linear discriminate models that differed on the number of neural features that were used as input and their origin. Whereas some models (enclosed by black boxes, Figure 5a) were derived from neural features extracted from a single brain region (STN / motor cortex) other models used neural features from both brain regions (STN & motor cortex, grey boxes). Of note, all models were *specific to each individual subject*, which was made possible by the large volume of data collected on each subject over many cycles of fluctuations in motor signs. The first model, used a 2 Hz window around subject specific peaks in spectral power in beta (12–30 Hz) or gamma (50–90 Hz) bands, or coherence in beta or gamma bands, for each contact montage within a hemisphere, as the neural features used to individually train the LD (linear discriminate) models (black boxes, Figure 5a). These LD models used a single neural feature to discriminate between "on" and "off" states as defined by the PKG. We trained several additional LD models to test if combining neural features within a single recording location (STN/MC) across spectral peaks (STN and Gamma) yielded performance gains (Figure 5a, rightmost black boxes). These models had four neural features as input (two contacts pairs and two spectral peaks – gamma and beta for each recording site (STN/MC). An additional LD model was trained using all possible coherence pairs between STN and MC using both spectral peaks (8 neural features per patient and hemisphere, leftmost grey box). Finally, the last LDA model was trained for each hemisphere, on the *combination* of all spectral power and coherence features (16 neural features) in beta and gamma bands, combining contact montages at both STN and cortical recording sites and coherence and power features to learn the model, rather than each pair/frequency band separately (rightmost grey box, Figure 5a).

All LD models (individual features and combined features) were computed and tested using a stratified 5-fold cross validation (e.g. we trained our model on 4/5's of the data and tested the model's predictions on the remaining 1/5 of the data). The resulting linear discriminant was used in a receiver-operator curve (ROC) analysis, and the mean area under the curve (AUC) was computed (individual points in Figure 5a). This process ensures that no test data were used in order to learn the model[11]. In addition to cross validation, we stratified the data which insures balanced representation of each class across the train and test sets. To assess

Author Manuscript Author Manuscript Author Manuscript Author Manuscript

the statistical significance of each LD measurement we used non-parametric methods and repeated each analysis 10000 times using shuffled labels, computed a p-value for each test by comparing the non-parametric distribution with the AUC derived from the non-shuffled labels. Significance was assessed at alpha 0.05 level, corrected for multiple comparisons using the Bonferroni method across all tests. Further details on use of within subjects modelling, and avoidance of overfitting, are provided in Supplemental Information.

Unsupervised clustering.

In order to perform unsupervised clustering to test whether states are separable without a-priori knowledge of the number of clusters or the location of peaks in the beta frequency, the average power in known physiological ranges (delta 1–4Hz, theta 4–8Hz, alpha 8 −13Hz, low beta 13–20Hz, high beta 20–30Hz, low gamma 30–50Hz, high gamma 50–90Hz), and their coherence spectra were fed into a clustering detection algorithm[12]. This algorithm does not require specifying the number of clusters (unlike k-means). We used the same temporal averaging as for LDA analysis (a 10 min window sampled every 2 min). We tested a second clustering approach that relies on capturing known physiological events in clinic and using them as a template to classify at-home data. These states have been well defined in-clinic and correlate with motor impairment in PD but it is unknown if they would be recapitulated in the home environment. We computed the normalized spectral power from a two min recording in-clinic in which patients were 12 hr off medication or following a therapeutic dose of levodopa). We used each in-clinic state spectrum as a template and classified each at-home PSD based on the smallest Euclidian distance to each of the two in-clinic templates.

Testing embedded adaptive stimulation.

Embedded adaptive DBS was implemented at home using a linear detector in “dual threshold” mode. Stimulation changed adaptively between upper and lower limits, preset by clinicians, when a neural signal crossed one of two preset thresholds (Figure 6). The “mental model” for the adaptive algorithms was to allow stimulation to change based on medication cycles, as tracked by neural biomarkers of “off” or “on” states, so as to allow more stimulation when in an “off’ state and less in an “on” state. This goal was to improve bradykinesia control in off states while reducing stimulation-induced dyskinesia in the on-state. Two types of neural control were tested in two subjects, one utilizing subthalamic beta band activity (RCS03), the other utilizing cortical gamma band activity (RCS01). For each, stimulation amplitude was changed only when the neural biomarker amplitude dropped below the lower threshold or exceeded the upper threshold; stimulation amplitude was held constant when the biomarker was between the thresholds. Stimulation changes occurred at ramp rates customized for each algorithm. Active recharge was used during stimulation with sense blanking whose duration was customized to each algorithm. We used the onboard (high pass (HPF) filter set at 0.85 Hz and two low pass filters (LPF) at 100 Hz – one before and one after amplification. The sampling rate was 250 Hz, and the FFT size was 256 points (1024ms of data). Each FFT interval was 500 ms and twenty FFT’s were averaged (10 s of data) in a non-moving average such that the detector made a “decision” about stimulation state every 10 s. The onset and termination timers (time requiring the control signal to be above or below the threshold for a certain amount of time to affect stimulation change) were set at zero, but the state change blanking was set at 2.5 s (lockout period for any additional

Author Manuscript Author Manuscript Author Manuscript Author Manuscript

state change resulting from the neural signal crossing one of the two preset thresholds). The settings for adaptive sessions were uploaded to the patients' computer remotely (with supervision from a neurologist on a video link). Patients performed their activities of daily living for 8 hr at home during the adaptive trial.

Home testing was done for one day for RCS03 and four days for RCS01, and compared with clinically optimized standard (unvarying) DBS for one day for RCS03 and four days for RCS01. (RCS 03 was unable to tolerate unvarying DBS amplitude for more than one day). Assessments were done for RCS01 (based on all eight days of testing) using both subjective measures (motor diaries) and objective measures (the PKG monitor). PKG two minute scores were parsed into "off", "on" and "on with dyskinesia" (Figure 6d). Adaptive DBS was only turned on during the waking hours. Additional details on settings for adaptive DBS and for algorithm risk management are provided in Supplemental Information. Further information on experimental design and inclusion criteria are available in the Life Sciences Reporting Summary linked to this article.

Author Manuscript Author Manuscript Author Manuscript Author Manuscript

Extended Data

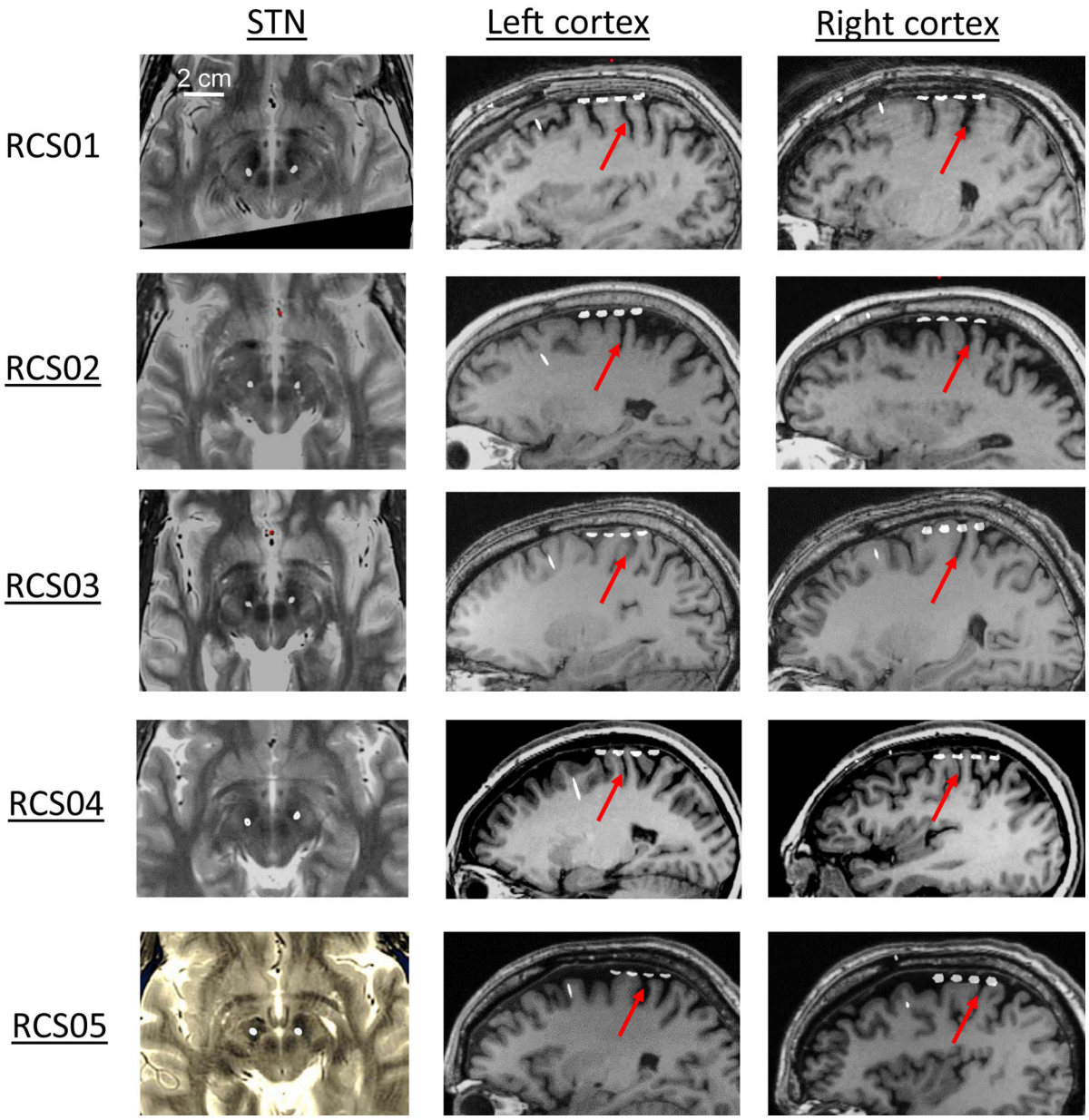

Extended Data Figure 1. Localization of leads in subthalamic nucleus and over precentral gyrus: all subjects.

Lead locations in all five subjects, from postoperative CT scan, computationally fused with the preoperative planning MRI. The contacts appear in white (CT artifacts from their metal content). Left column, STN leads on axial T2 weighted MRI passing through the midbrain-diencephalic junction. The STN and red nuclei are regions of T2 hypointensity. Middle and right column, quadripolar subdural paddle leads on T1 weighted MRI (oblique sagittal passing through long axis of the lead array). Red arrow indicates central sulcus. Either contact 9 (subjects 1,2,3,5) or contact 10 (subject 4) is positioned at the posterior margin of precentral gyrus (primary motor area). Horizontal white line represents 2cm.

Author Manuscript Author Manuscript Author Manuscript Author Manuscript

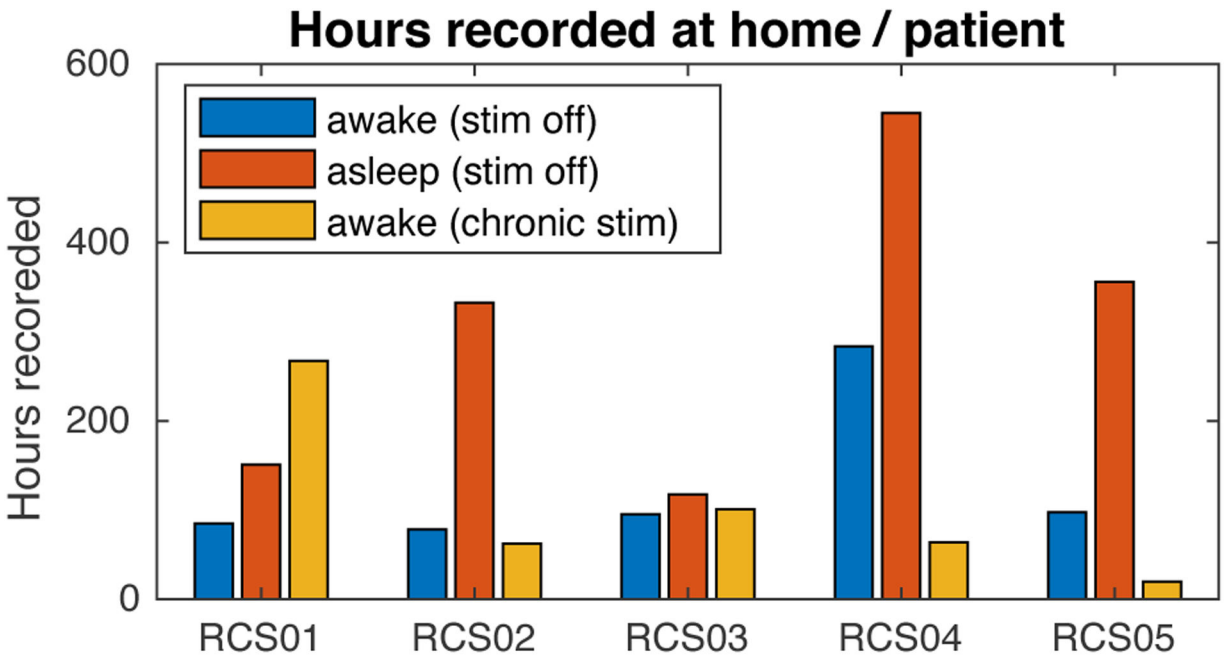

Extended Data Figure 2. Over 2,600 hours of motor cortex and basal ganglia field potentials streamed in home environment

Number of hours of eight-channel neural data recorded by each patient while awake and while asleep, prior to initiating therapeutic stimulation and also while awake during chronic therapeutic stimulation. Here, “asleep” was defined as 10 PM to 8 AM.

Author Manuscript Author Manuscript Author Manuscript Author Manuscript

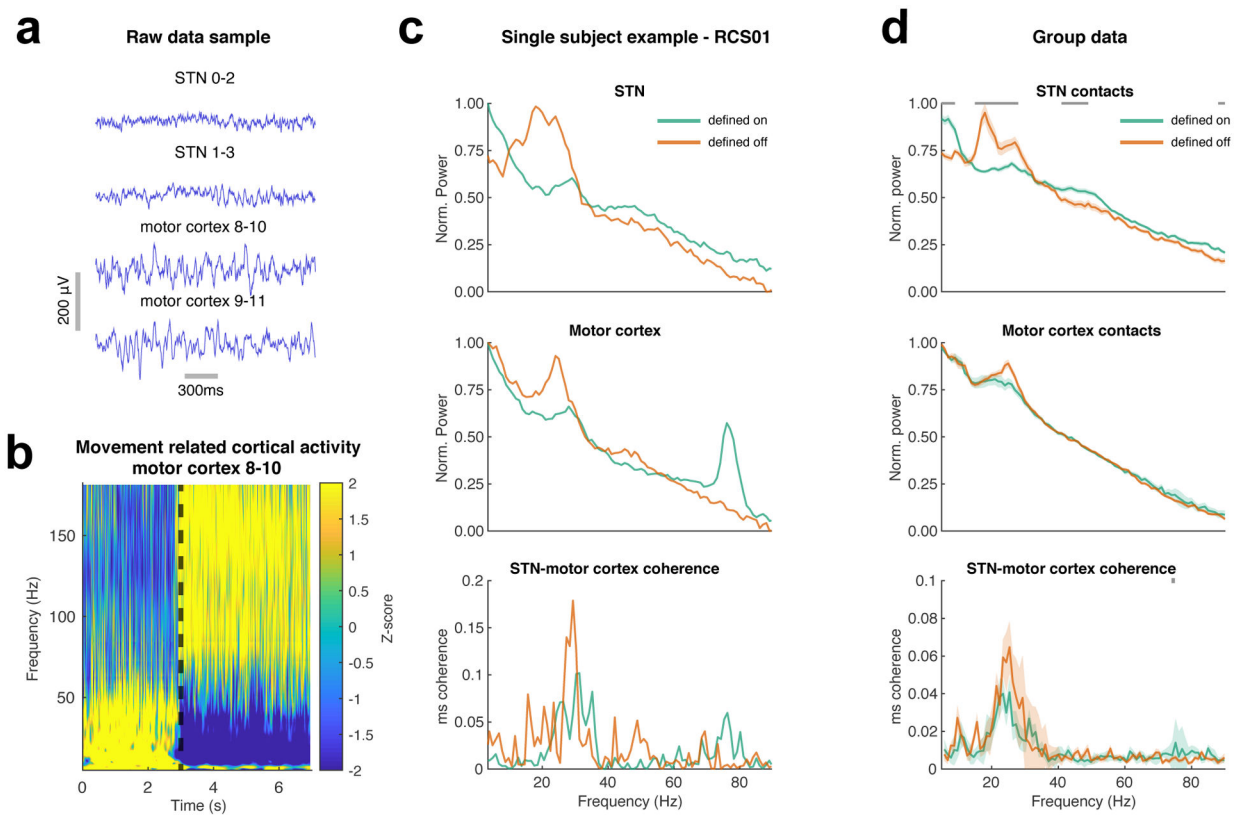

Extended Data Figure 3. Brief in-clinic recordings demonstrate effects of leovodopa and movement.

a, Example field potentials recorded from right hemisphere, STN (top) and motor cortex (bottom). Horizontal grey line represents 300ms, vertical line is 200 µV. **b**, Example spectrogram of cortical activity (bipolar recordings contacts 8–10) showing canonical movement-related alpha-beta band (8–35 Hz) decrease, and broadband (50–200 Hz) increase, consistent with placement over sensorimotor cortex (from RCS04), recorded 27 days post-implantation (sampling rate 500 Hz). Dotted vertical line is the onset of movement. Color scale is z-scored. **c**, Example power spectra of STN and motor cortex field potentials, and coherence between them, showing oscillatory profile of off-levodopa (red) and on-levodopa (green) states (patient RCS01), from 30 second recordings. **d**, Average PSD and coherence plots across both hemispheres, both recording montages, and all five patients. STN beta amplitude is reduced in the on-medication state. Horizontal bar shows frequency bands that had significant differences between states ($p<0.05$, two sided, Bonferroni corrected). Shading in group data represents standard error of the mean.

Author Manuscript Author Manuscript Author Manuscript Author Manuscript

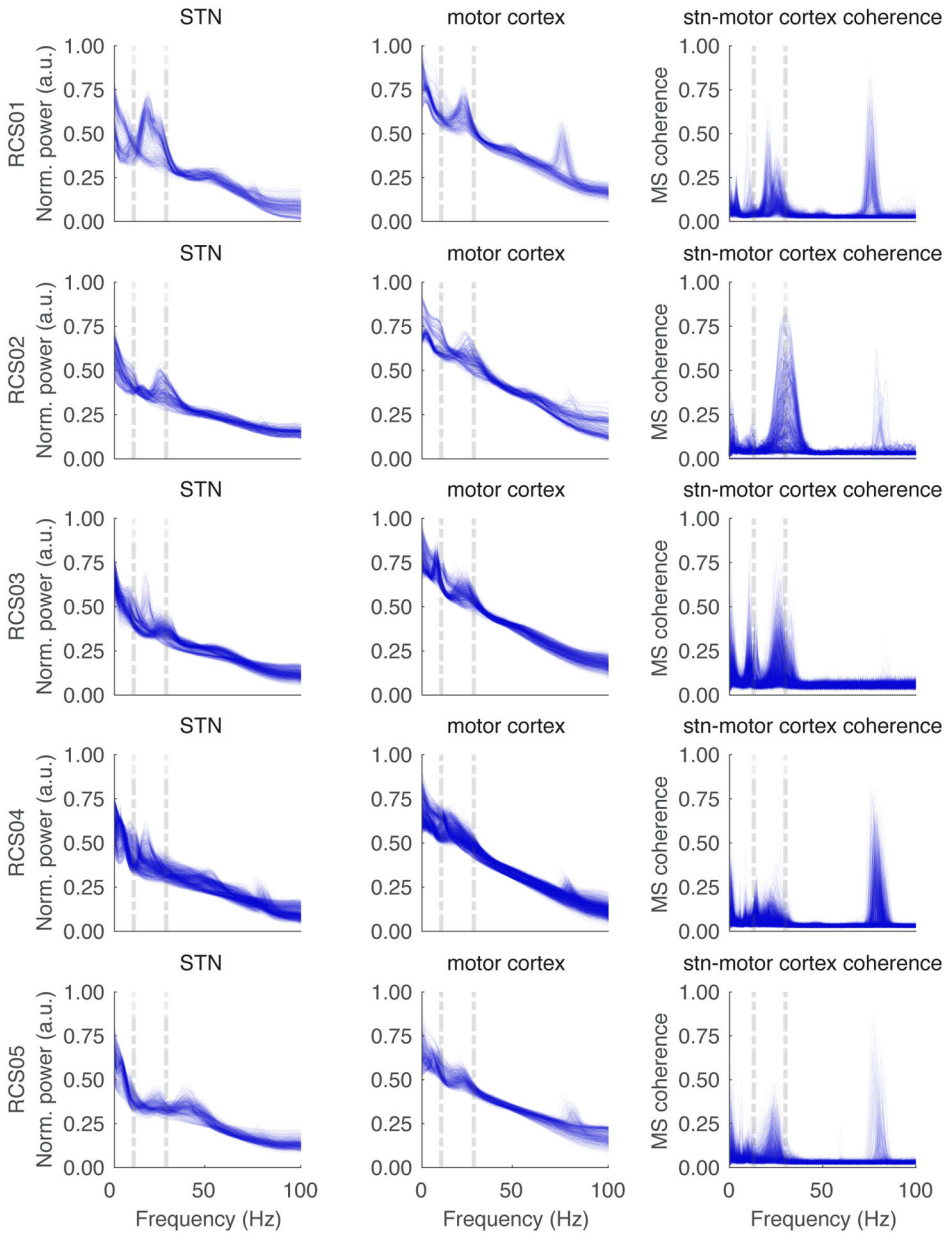

Extended Data Figure 4. Power spectra used for Parkinsonian motor state decoding: all subjects.

Superimposed STN and motor cortex power spectra (left two columns) and STN-motor cortex coherence (right column) from averaged 10 minute nonoverlapping data segments, showing all data collected during home recordings that were used for motor state decoding (Figures 4,5). Data are for all five subjects from both hemispheres, prior to starting therapeutic stimulation. Both recording channels for each target (0–2 and 1–3 for STN, 8–10 and 9–11 for motor cortex) are represented. Each row shows all data from one study subject. Vertical dotted lines at 13 and 30 Hz demarcate the beta band, for visual clarity.

Author Manuscript Author Manuscript Author Manuscript Author Manuscript

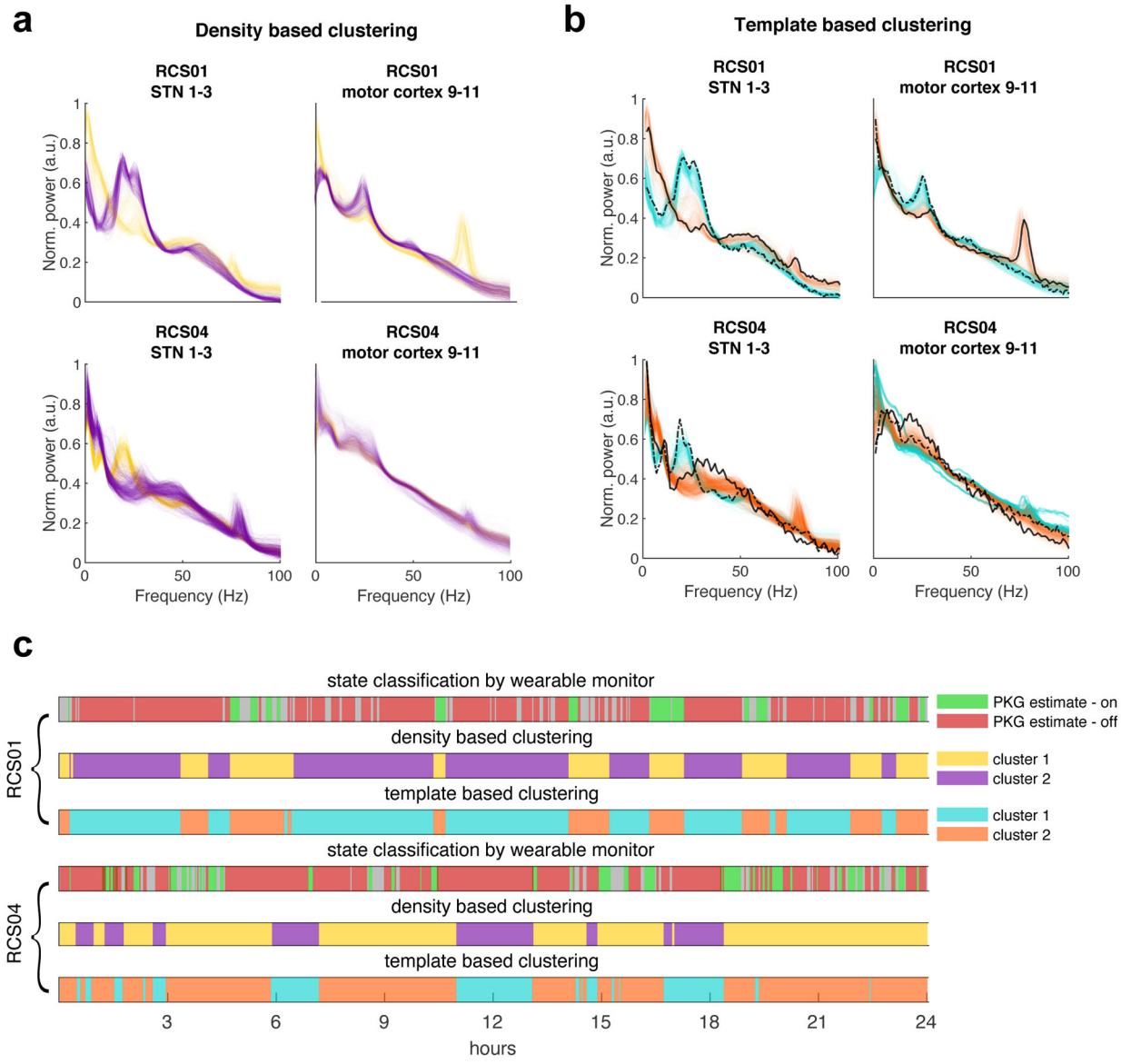

Extended Data Figure 5. Unsupervised clustering segregates neural data into specific behavioral states.

Example patients are RCS01 and RCS04. All raw data (recorded in the awake state) were segregated using unsupervised clustering algorithms with two different paradigms: **a,** Unsupervised clustering using a density based method[25]. **b,** Clustering of PSDs based on template PSDs from in clinic recording in defined on/off medication states. Black lines are the template PSD's (dotted = off medication, solid = on medication). **c,** Concordance with brain states derived from wearable monitor. Barcodes compare motor state estimates derived from the wearable monitors, with the clusters derived from type of clustering algorithm (24-hour data sample).

Author Manuscript Author Manuscript Author Manuscript Author Manuscript

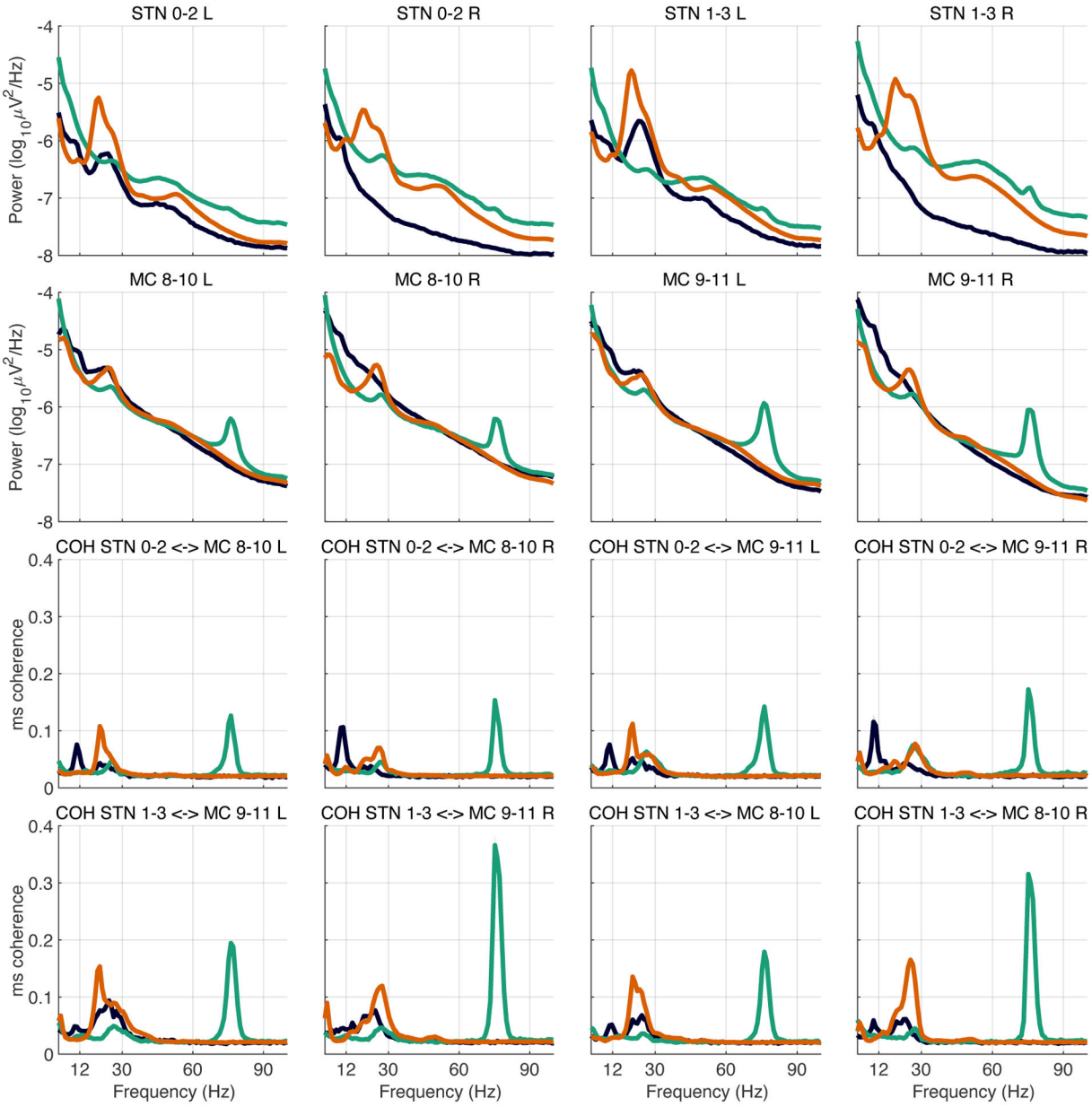

Extended Data Figure 6: Sleep strongly affects neural biomarkers.

Sleep strongly affects neural biomarkers. Example data from RCS01,220 hours of recording during which states were segregated by bilateral wearable monitors. PKG monitor classifications were used to segregate PSD's (10 minute averages) to "off" (orange), "on" (green) and "sleep" (black) states. Note that the "sleep" state is characterized by profound reductions in STN beta band oscillations, STN broadband activity, and all gamma band oscillations, but increases in low frequency (<12 Hz) activity in cortex, and in most of the pairwise cortex-STN coherence plots. STN= subthalamic nucleus, MC=motor cortex, coh=coherence between STN and motor cortex.

Author Manuscript
Author Manuscript
Author Manuscript
Author Manuscript

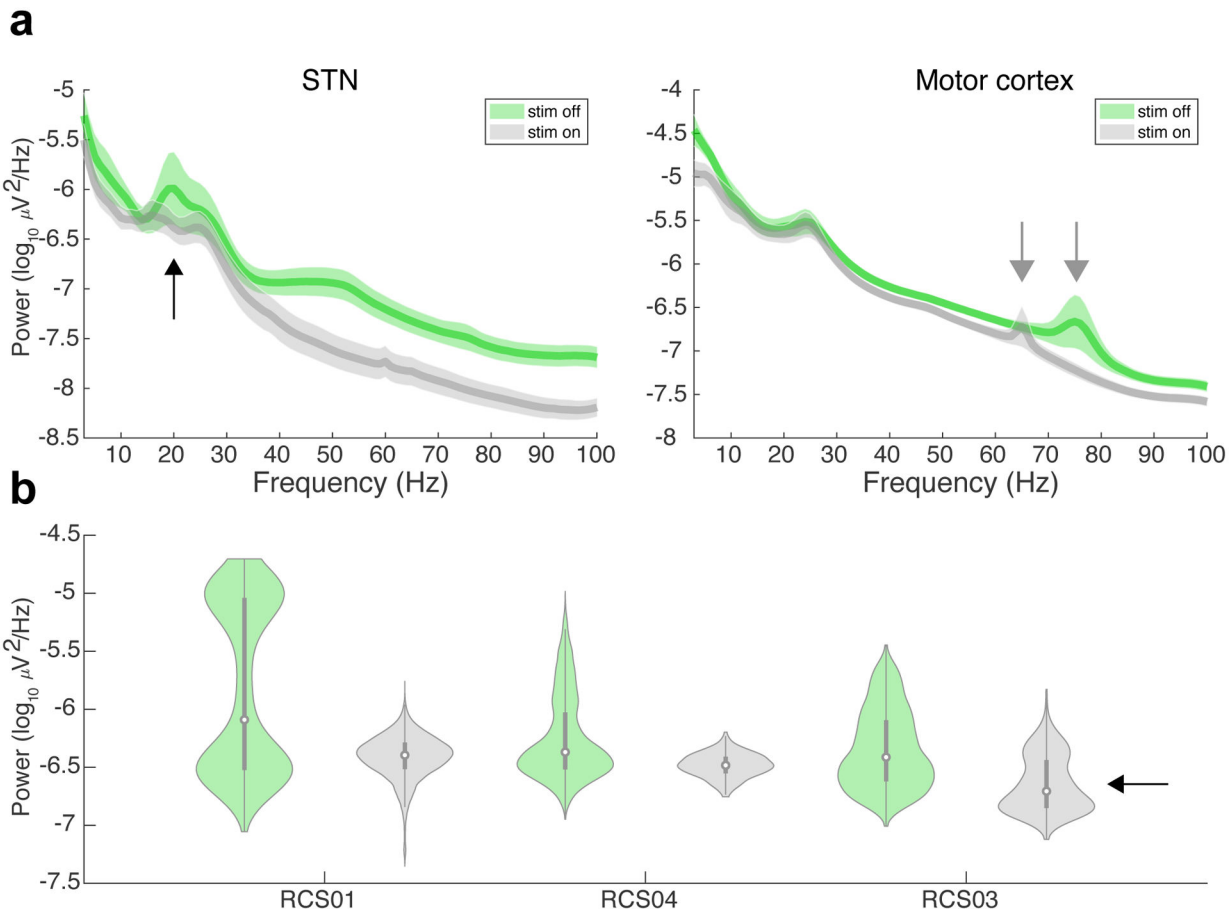

Extended Data Figure 7. Effects of standard therapeutic DBS on oscillatory activity.

Power spectrum averaged over all off-stimulation and on-stimulation data in one subject (RCS01), over a total of 352 hours of recording at home during waking hours. Left plot, chronic recording from same quadripolar STN contact array (sense contacts 0–2) as utilized for therapeutic stimulation, with reduction in beta band activity during stimulation ($p<0.001$, two sided) (arrow). Right plot, simultaneously collected data recorded from motor cortex (sense contacts 9–11), shows stimulation-induced frequency shift in gamma activity[13] and no concomitant change in cortical beta band activity. Average PSDs for all 10 min data segments segregated by off stimulation (green), and on stimulation (gray). Shading represents one standard deviation. Differences in filters implemented during stimulation may explain the baseline shifts above 30 Hz. **b,** Violin plots showing the average beta power (5 Hz window surrounding peak) off/on chronic stimulation in three subjects (895 total hours of recording). In two examples, chronic open loop STN DBS both reduces median STN beta band activity, and collapses the biomodal distribution of beta activity to a unimodal one. In one example (RCS03 L side), chronic open loop DBS also reduces median STN beta band activity, but the distribution remains bimodal (arrow), suggesting persistence of motor fluctuations during DBS.

Author Manuscript Author Manuscript Author Manuscript Author Manuscript

Supplementary Material

Refer to Web version on PubMed Central for supplementary material.

Acknowledgements:

The authors would like to thank Lauren Hammer for critical reading of the manuscript and Maria Olaru for proofreading. The work was funded by NIH grant UH3NS100544 (PI: Starr).

References

1. Lozano AMet al.Deep brain stimulation: current challenges and future directions. Nature reviews. Neurology15, 148–160 (2019). [PubMed: 30683913]
2. Voytek B & Knight RT Dynamic network communication as a unifying neural basis for cognition, development, aging, and disease. Biological psychiatry 77, 1089–1097 (2015). [PubMed: 26005114]
3. Ritaccio ALet al.Proceedings of the Eighth International Workshop on Advances in Electrocorticography. Epilepsy & behavior : E&B64, 248–252 (2016).
4. Starr PATotally Implantable Bidirectional Neural Prostheses: A Flexible Platform for Innovation in Neuromodulation. Front Neurosci12, 619 (2018). [PubMed: 30245616]
5. Sun FT & Morrell MJ The RNS System: responsive cortical stimulation for the treatment of refractory partial epilepsy. Expert review of medical devices 11, 563–572 (2014). [PubMed: 25141960]
6. Meidahl ACet al.Adaptive Deep Brain Stimulation for Movement Disorders: The Long Road to Clinical Therapy. Mov Disord32, 810–819 (2017). [PubMed: 28597557]
7. Rouse AGet al.A chronic generalized bi-directional brain-machine interface. Journal of neural engineering8, 036018 (2011). [PubMed: 21543839]
8. Swann NCet al.Chronic multisite brain recordings from a totally implantable bidirectional neural interface: experience in 5 patients with Parkinson's disease. Journal of neurosurgery128, 605–616 (2018). [PubMed: 28409730]
9. Stanslaski Set al.A Chronically Implantable Neural Coprocessor for Investigating the Treatment of Neurological Disorders. IEEE transactions on biomedical circuits and systems12, 1230–1245 (2018). [PubMed: 30418885]
10. Kremen Vet al.Integrating Brain Implants With Local and Distributed Computing Devices: A Next Generation Epilepsy Management System. IEEE journal of translational engineering in health and medicine6, 2500112 (2018). [PubMed: 30310759]
11. Wozny TAet al.Effects of hippocampal low-frequency stimulation in idiopathic non-human primate epilepsy assessed via a remote-sensing-enabled neurostimulator. Experimental neurology294, 68–77 (2017). [PubMed: 28495218]
12. Brittain JS & Brown P Oscillations and the basal ganglia: motor control and beyond. NeuroImage 85 Pt 2, 637–647 (2014). [PubMed: 23711535]
13. Swann NCet al.Gamma Oscillations in the Hyperkinetic State Detected with Chronic Human Brain Recordings in Parkinson's Disease. J Neurosci36, 6445–6458 (2016). [PubMed: 27307233]
14. de Hemptinne Cet al.Exaggerated phase-amplitude coupling in the primary motor cortex in Parkinson disease. Proceedings of the National Academy of Sciences of the United States of America110, 4780–4785 (2013). [PubMed: 23471992]
15. Silberstein Pet al.Cortico-cortical coupling in Parkinson's disease and its modulation by therapy. Brain128, 1277–1291 (2005). [PubMed: 15774503]
16. Little Set al.Adaptive deep brain stimulation in advanced Parkinson disease. Annals of neurology74, 449–457 (2013). [PubMed: 23852650]
17. Little Set al.Adaptive deep brain stimulation for Parkinson's disease demonstrates reduced speech side effects compared to conventional stimulation in the acute setting. Journal of neurology, neurosurgery, and psychiatry87, 1388–1389 (2016).

Author Manuscript Author Manuscript Author Manuscript Author Manuscript

18. Velisar Aet al.Dual threshold neural closed loop deep brain stimulation in Parkinson disease patients. Brain stimulation12, 868–876 (2019). [PubMed: 30833216]
19. Swann NCet al.Adaptive deep brain stimulation for Parkinson's disease using motor cortex sensing. Journal of neural engineering15, 046006 (2018). [PubMed: 29741160]
20. Herron JAet al.Chronic electrocorticography for sensing movement intention and closed-loop deep brain stimulation with wearable sensors in an essential tremor patient. Journal of neurosurgery127, 580–587 (2017). [PubMed: 27858575]
21. Panov Fet al.Intraoperative electrocorticography for physiological research in movement disorders: principles and experience in 200 cases. Journal of neurosurgery126, 122–131 (2017). [PubMed: 26918474]
22. Horne MK, McGregor S & Bergquist F An objective fluctuation score for Parkinson's disease. PloS one 10, e0124522 (2015). [PubMed: 25928634]
23. Timmermann Let al.The cerebral oscillatory network of parkinsonian resting tremor. Brain126, 199–212 (2003). [PubMed: 12477707]
24. Qasim SEet al.Electrocorticography reveals beta desynchronization in the basal ganglia-cortical loop during rest tremor in Parkinson's disease. Neurobiology of disease (2015).
25. Graat Iet al.Is deep brain stimulation effective and safe for patients with obsessive compulsive disorder and comorbid bipolar disorder?Journal of affective disorders264, 69–75 (2019). [PubMed: 31846903]
26. Huang Y, Cheeran B, Green AL, Denison TJ & Aziz TZ Applying a Sensing-Enabled System for Ensuring Safe Anterior Cingulate Deep Brain Stimulation for Pain. Brain sciences 9 (2019).
27. Frizon LAet al.Deep Brain Stimulation for Pain in the Modern Era: A Systematic Review. Neurosurgery (2019).
28. Fasano A & Helmich RC Tremor habituation to deep brain stimulation: Underlying mechanisms and solutions. Mov Disord 34, 1761–1773 (2019). [PubMed: 31433906]
29. Lo MC & Widge AS Closed-loop neuromodulation systems: next-generation treatments for psychiatric illness. International review of psychiatry 29, 191–204 (2017). [PubMed: 28523978]
30. Tinkhauser Get al.The modulatory effect of adaptive deep brain stimulation on beta bursts in Parkinson's disease. Brain140, 1053–1067 (2017). [PubMed: 28334851]
31. Kirkby LAet al.An Amygdala-Hippocampus Subnetwork that Encodes Variation in Human Mood. Cell175, 1688–1700e1614 (2018). [PubMed: 30415834]
32. Molina Ret al.Report of a patient undergoing chronic responsive deep brain stimulation for Tourette syndrome: proof of concept. Journal of neurosurgery, 1–7 (2017).
33. Quinn EJet al.Beta oscillations in freely moving Parkinson's subjects are attenuated during deep brain stimulation. Mov Disord30, 1750–1758 (2015). [PubMed: 26360123]
34. Syrkin-Nikolau Jet al.Subthalamic neural entropy is a feature of freezing of gait in freely moving people with Parkinson's disease. Neurobiology of disease108, 288–297 (2017). [PubMed: 28890315]
35. Neumann WJet al.Long term correlation of subthalamic beta band activity with motor impairment in patients with Parkinson's disease. Clin Neurophysiol128, 2286–2291 (2017). [PubMed: 29031219]
36. Molina Ret al.Neurophysiological Correlates of Gait in the Human Basal Ganglia and the PPN Region in Parkinson's Disease. Frontiers in human neuroscience14, 194 (2020). [PubMed: 32581744]
37. Van Gompel JJet al.Anterior nuclear deep brain stimulation guided by concordant hippocampal recording. Neurosurgical focus38, E9 (2015).
38. Vansteensel MJet al.Fully Implanted Brain-Computer Interface in a Locked-In Patient with ALS. The New England journal of medicine375, 2060–2066 (2016). [PubMed: 27959736]
39. Koeglsperger T, Mehrkens JH & Botzel K Bilateral double beta peaks in a PD patient with STN electrodes. Acta Neurochir (Wien) (2020).
40. de Hemptinne Cet al.Therapeutic deep brain stimulation reduces cortical phase-amplitude coupling in Parkinson's disease. Nature neuroscience18, 779–786 (2015). [PubMed: 25867121]

Author Manuscript Author Manuscript Author Manuscript Author Manuscript

41. Cole SRet al.Nonsinusoidal Beta Oscillations Reflect Cortical Pathophysiology in Parkinson's Disease. J Neurosci37, 4830–4840 (2017). [PubMed: 28416595]

Methods Only References

1. Postuma RBet al.MDS clinical diagnostic criteria for Parkinson's disease. Mov Disord30, 1591–1601 (2015). [PubMed: 26474316]
2. Swann NCet al.Chronic multisite brain recordings from a totally implantable bidirectional neural interface: experience in 5 patients with Parkinson's disease. Journal of neurosurgery128, 605–616 (2018). [PubMed: 28409730]
3. Kremen Vet al.Integrating Brain Implants With Local and Distributed Computing Devices: A Next Generation Epilepsy Management System. IEEE journal of translational engineering in health and medicine6, 2500112 (2018). [PubMed: 30310759]
4. Stanslaski Set al.A Chronically Implantable Neural Coprocessor for Investigating the Treatment of Neurological Disorders. IEEE transactions on biomedical circuits and systems12, 1230–1245 (2018). [PubMed: 30418885]
5. Pourfar Met al.Assessing the microlesion effect of subthalamic deep brain stimulation surgery with FDG PET. Journal of neurosurgery110, 1278–1282 (2009). [PubMed: 19301972]
6. Mann JMet al.Brain penetration effects of microelectrodes and DBS leads in STN or GPi. Journal of neurology, neurosurgery, and psychiatry80, 794–797 (2009).
7. de Hemptinne Cet al.Therapeutic deep brain stimulation reduces cortical phase-amplitude coupling in Parkinson's disease. Nature neuroscience18, 779–786 (2015). [PubMed: 25867121]
8. Griffiths RIet al.Automated assessment of bradykinesia and dyskinesia in Parkinson's disease. J Parkinsons Dis2, 47–55 (2012). [PubMed: 23939408]
9. Braybrook Met al.An Ambulatory Tremor Score for Parkinson's Disease. J Parkinsons Dis6, 723–731 (2016). [PubMed: 27589540]
10. Horne MK, McGregor S & Bergquist F An objective fluctuation score for Parkinson's disease. PloS one 10, e0124522 (2015). [PubMed: 25928634]
11. Varoquaux Get al.Assessing and tuning brain decoders: Cross-validation, caveats, and guidelines. NeuroImage145, 166–179 (2017). [PubMed: 27989847]
12. Rodriguez A & Laio A Machine learning. Clustering by fast search and find of density peaks. Science (New York, N.Y 344, 1492–1496 (2014).

Author Manuscript Author Manuscript Author Manuscript Author Manuscript

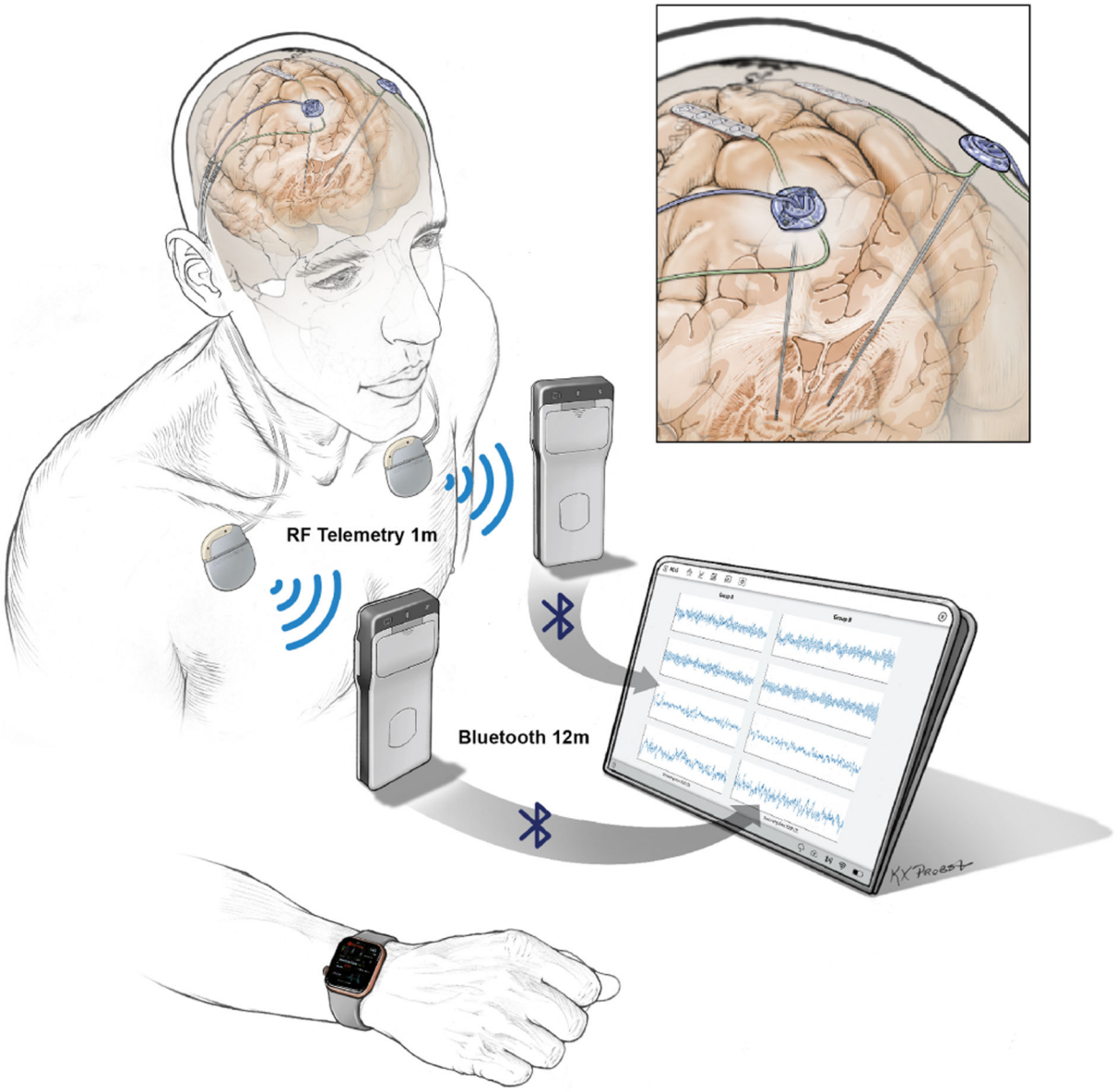

Figure 1. Configuration of implanted hardware and method of data streaming.

Quadripolar leads were placed bilaterally into the subthalamic nuclei and in the subdural space over precentral gyri to cover primary motor cortex (inset provides zoomed-in view). Each DBS lead and cortical paddle pair were connected via tunneled lead extenders to the ipsilateral Summit RC+S bidirectional implantable pulse generator (IPG), placed in a pocket over the pectoralis muscle. Each RC+S uses radiofrequency telemetry in the medical implant communication spectrum (MICS) band to wirelessly communicate with a pocket sized relay device, usually worn on the patient. The relay devices transmit by Bluetooth to a single small Windows-based tablet at a distance of up to 12 m, allowing sensing of local field potentials from up to four bipolar electrode pairs for up to 30 hours per IPG, before recharge is needed. Custom software on the tablet allows remote updating of device streaming parameters or adjustment of embedded adaptive DBS algorithms, at

home. Data from a wristwatch-style actigraphy monitor (Parkinson's Kinetograph, Global Kinetics) are downloaded to a server that is synchronized off-line with neural recordings for brain-behavior correlations. RF, radio frequency.

Author Manuscript Author Manuscript Author Manuscript Author Manuscript

Author Manuscript Author Manuscript Author Manuscript Author Manuscript

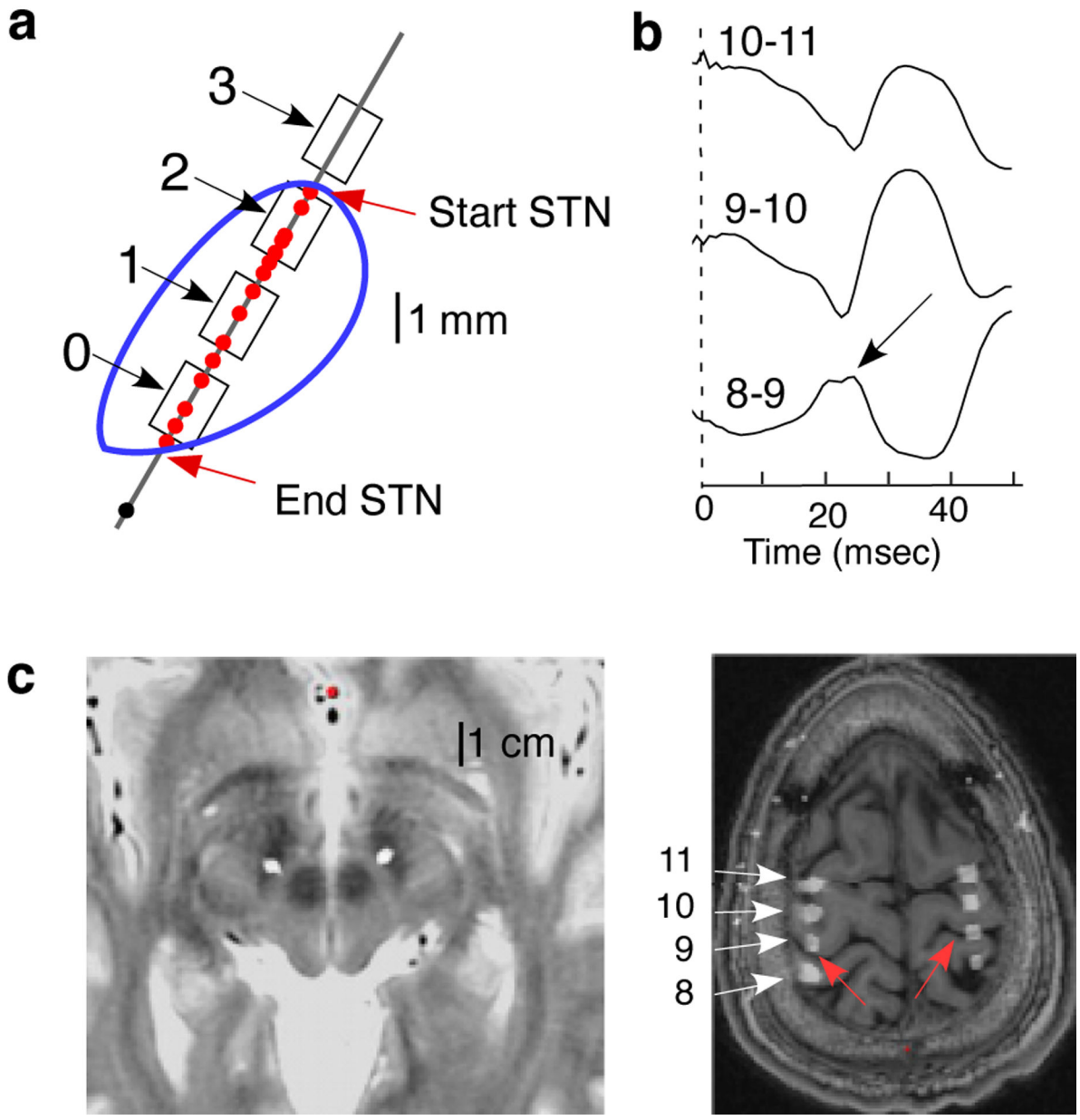

Figure 2. Anatomic and physiological localization of subthalamic and cortical leads (example from RCS04).

a, Localization of STN contacts with respect to the borders of STN (outlined in blue) as defined by microelectrode mapping. The microelectrode map (green line) shows the borders of STN as defined by cells (red dots) that have canonical STN single unit discharge patterns and rates. The intended depth of the DBS lead is determined by this map, and contact numbers are labelled. The middle contacts (1 and 2) are within the dorsal 4 mm of STN (motor territory). The black dot is a cell in substantia nigra, pars reticulata. b, Somatosensory evoked potential (from stimulation of the median nerve) recorded from the subdural paddle lead, montaged for three overlapping contact pairs. Reversal of the N20 potential between pairs 8–9 and 9–10 (arrow) shows localization of contact 9 to primary motor cortex, consistent with subsequent imaging. c, Location of the leads from

Author Manuscript Author Manuscript Author Manuscript Author Manuscript

postoperative CT computationally fused with the preoperative planning MRI. Left, STN leads on axial T2 weighted MRI which shows the STN as a region of T2 hypointensity. Right, quadripolar subdural paddle contacts on axial T1 weighted MRI showing relationship to central sulcus (red arrows) and numbering of contacts (white arrows).

Author Manuscript Author Manuscript Author Manuscript Author Manuscript

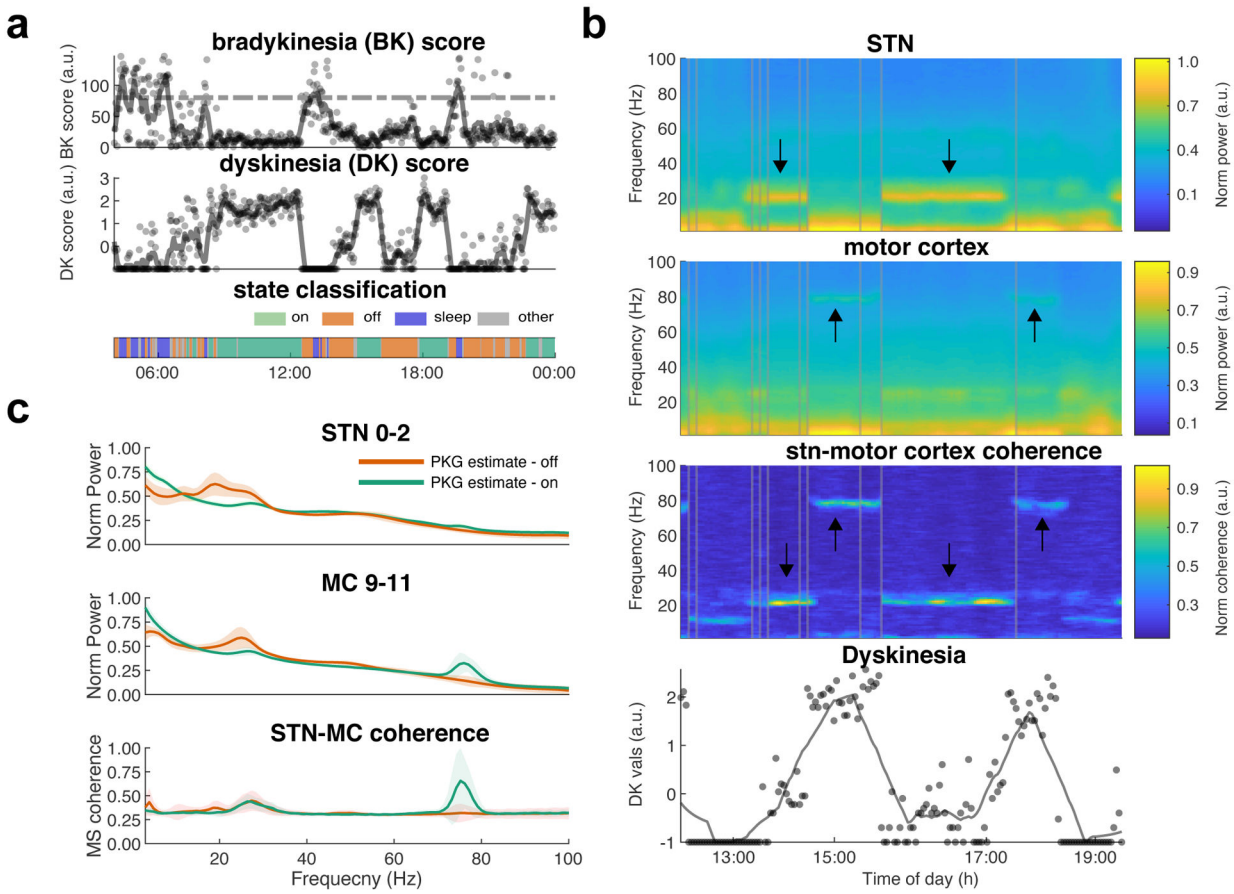

Figure 3. Decoding motor fluctuations from long duration recordings at home, single subject example (RCS01).

a, Data from wearable Personal KinetiGraph (PKG) monitor scores for bradykinesia and dyskinesia in 10 minute intervals. Example from one day. Assignment of motor state is shown in the horizontal colored bar. **b,** Capturing transitions between immobile (off) and mobile/dyskinetic states. Top, spectrograms for STN and motor cortex, and STN-motor cortex coherence over a 7.5 hour period (all times PM). Arrows indicate frequency bands sensitive to on-off fluctuations. Grey vertical lines show areas where the recording was discontinuous and was concatenated. Bottom, PKG dyskinesia scores indicate four transitions between off (low dyskinesia) and on with dyskinesia (patient had severe fluctuations). These are associated with transitions in beta and gamma oscillatory activity. **c,** Power spectra of STN and motor cortex, and STN-motor cortex coherence for all awake data from patient RCS01, segregated by mobile (on) and immobile (off) states (categorized by PKG) and averaged. Grey dashed boxes represent canonical frequencies (alpha, beta, gamma) in which an oscillation was present (see methods) and a significant difference between states was observed using the Wilcoxon ranksum test (corrected for multiple comparisons). a.u.=arbitrary units, STN=subthalamic nucleus. MC = motor cortex. MS = magnitude squared. DK = dyskinesia. BK = bradykinesia.

Author Manuscript Author Manuscript Author Manuscript Author Manuscript

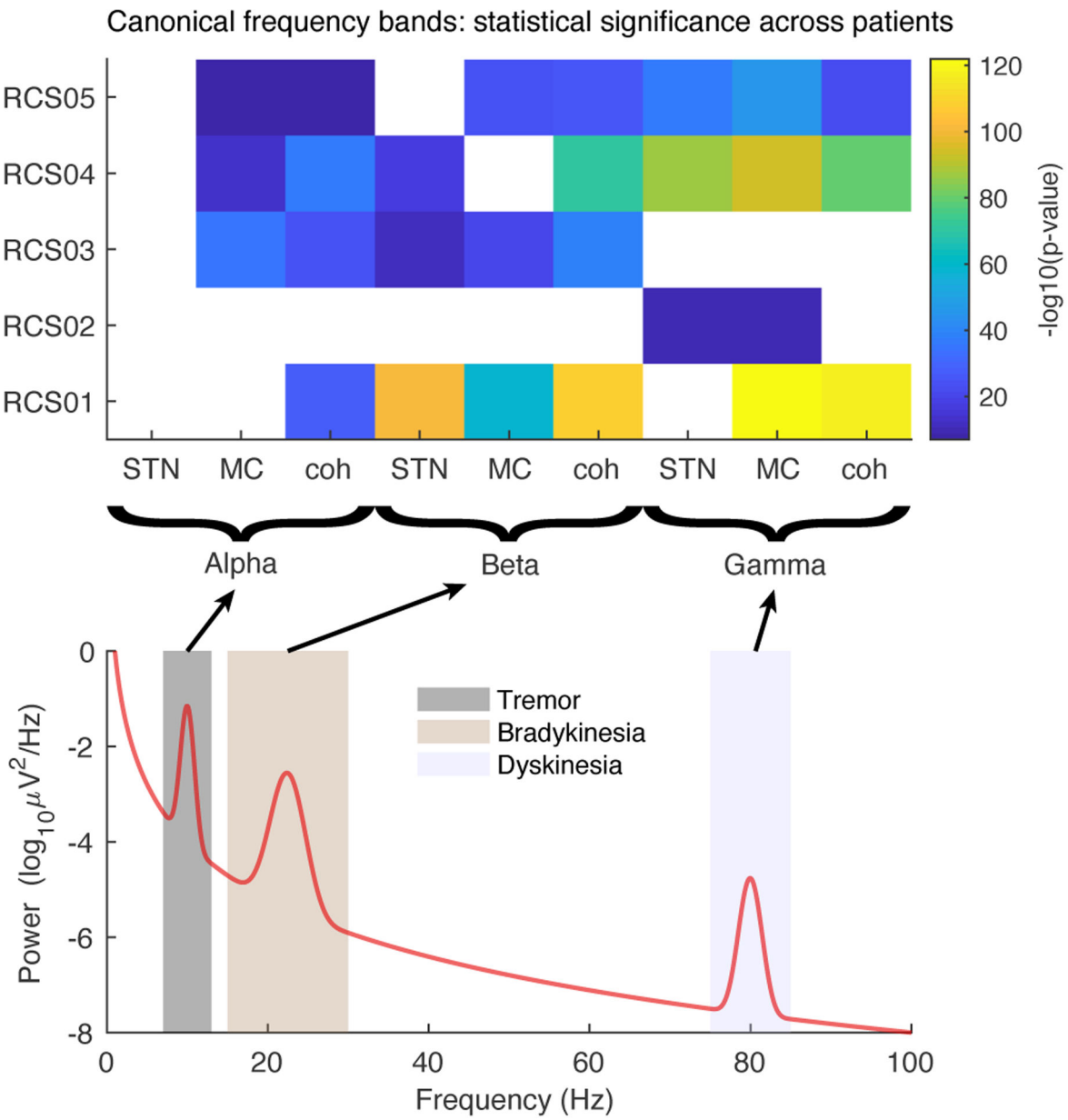

Figure 4. Personalized oscillatory fingerprints: statistical significance in defined frequency bands for all subjects.

Colorplot of p-values (two sided Wilcoxon rank-sum tests) evaluating if oscillatory power and coherence in canonical bands (alpha 8–12 Hz, beta 12–30 Hz, narrow band gamma 70–90 Hz) distinguishes between mobile vs immobile states (as determined by PKG monitor) for each patient and region. Colored squares represent areas in which the computed p-value survived multiple comparisons and a peak in the PSD was present (the *corrected* p-value equivalent for p=0.001 on this log scale is 4.68). Average PSD/coherence values from a 4 Hz window around peak were used for tests. Schematic below the colorplot illustrates spectral peaks at canonical frequencies that may be associated with specific motor signs. STN = subthalamic nucleus, MC = motor cortex, coh=coherence between STN and motor cortex.

Author Manuscript Author Manuscript Author Manuscript Author Manuscript

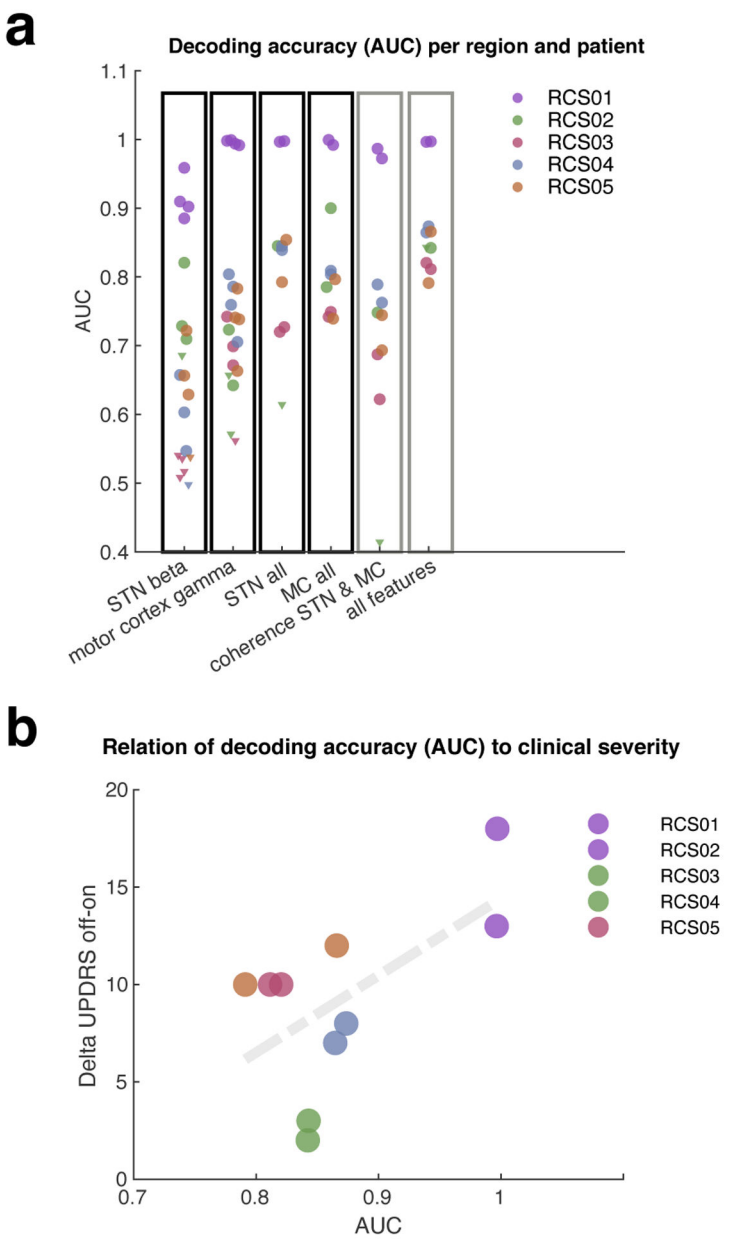

Figure 5. Contribution of specific features and recording sites to the decoding of movement state for all five subjects.

Decoding was done by fitting a linear discriminant (LD) to neural features with true labels coming from a wearable sensor (PKG watch). A LD model was learned for each feature (or combination of features) and the average area under the curve (AUC) was computed. **a**, AUC from receiver operator curve (ROC) analysis, showing that utilizing data from both STN and cortex better discriminates mobile and immobile states (as segregated by PKG scores), than either site alone. Each symbol in each column represents a single within-subjects model from a single hemisphere, computed in a variety of ways: From neural data derived from a single brain region (STN or cortex, data columns within solid black boxes) or from combinations of data from both brain regions (columns within grey boxes). For the two data columns on the left, separate LD models were constructed for

Author Manuscript Author Manuscript Author Manuscript Author Manuscript

each of two recording channels within the STN or the cortex (yielding 20 symbols, two for each hemisphere), and were also separated by frequency band utilized by the model (beta or gamma). For the other four columns, both recording channels, and both frequency bands were combined for each LD model (yielding 10 symbols, one for each hemisphere). Circles represent significant AUC measurements (tested non-parametrically) while triangles did not pass multiple comparison correction. Colors segregate all scores coming from the same patient. **b**, Correlation between decoding accuracy (using all features from **a,** far right data column) and the severity of motor fluctuations, estimated by the preoperative difference between the lateralized MDS-UPDRS part III scores for akinesia and rigidity, on-medication versus 12 hours off medication ($p = 0.065$ for linear regression line, one sided uncorrected). Neural data from RCS01 has the most accurate state decoding and the most severe motor fluctuations.

Author Manuscript Author Manuscript Author Manuscript Author Manuscript

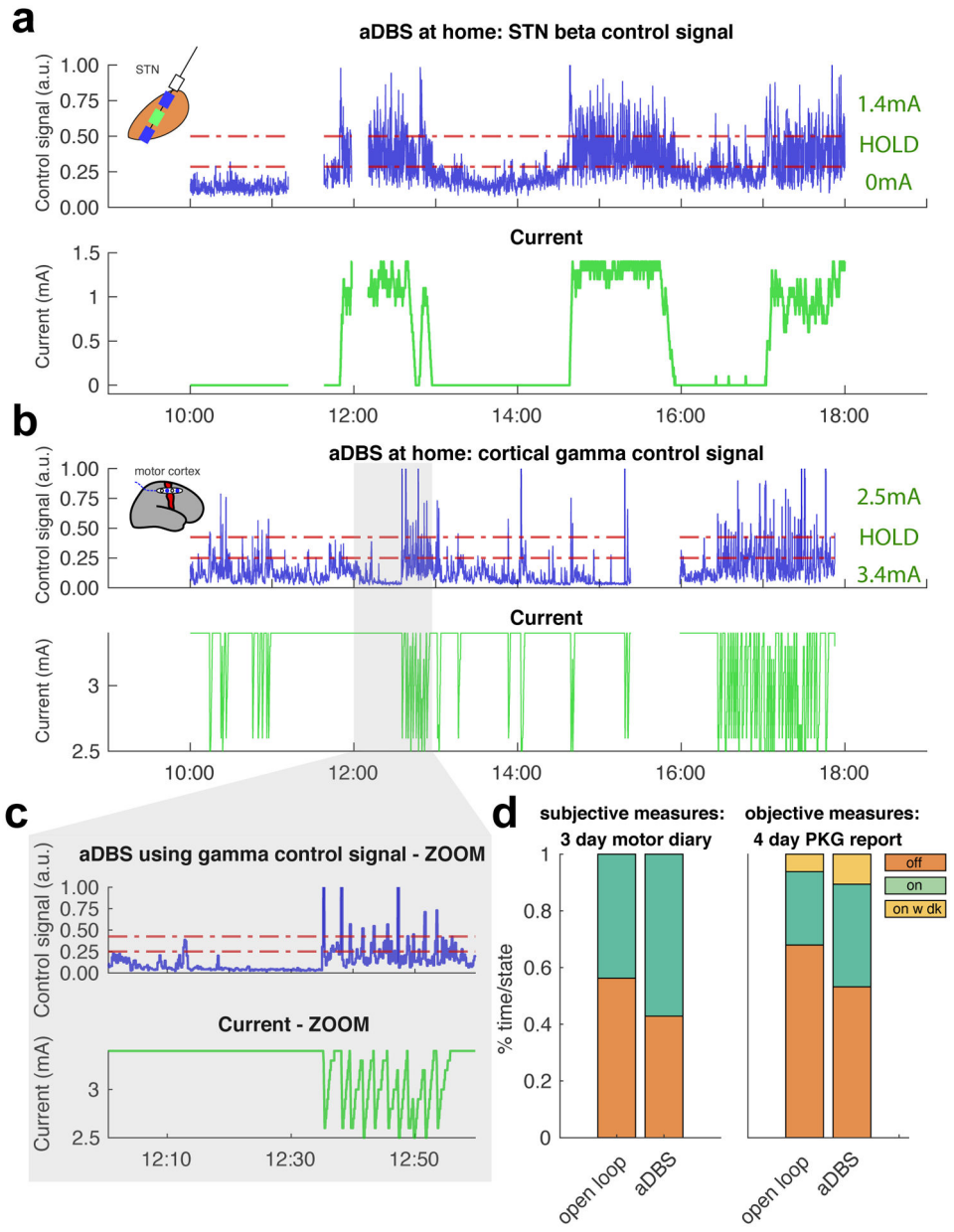

Figure 6: Adaptive DBS recorded at home using subcortical beta or cortical gamma control signals from two patients.

a and **b**, Neural data recording during two 8 hour sessions at home while running embedded adaptive STN DBS algorithms utilizing (a) subcortical STN beta band (RCS03) and (b) cortical gamma band (RCS01) as the control signals. Patients were at home undergoing activities of daily living on their habitual antiparkinsonian medications. Spectral power in the predefined frequency bands was computed on the device from the time domain signal, averaged and used to control stimulation. Blue plots show the neural control signals; green plots show the resulting stimulation current. Horizontal dotted lines on the control signal plots indicate upper and lower spectral power thresholds at which changes in stimulation amplitude were triggered. **a**, When the control signal is below the bottom threshold (indicating a risk a mobile state not requiring stimulation), current ramps down

Author Manuscript Author Manuscript Author Manuscript Author Manuscript

to 0mA. Current is held constant between thresholds, and ramps up to 1.4mA when the control signal is above the upper threshold. **b,** When the control signal is below the lower threshold current ramps to the highest amplitude (3.4mA). Between thresholds, current is held, and above the upper threshold, (indicating a risk for dyskinesia), current ramps down to 2.5mA. **c.** "Zoomed in" view of the plot in **b,** between noon and 1 pm, showing rapid current ramp down rates (to avoid or promptly arrest dyskinesia) and slower ramp up rates. **d.** Subjective and Objective evaluation of motor function for adaptive DBS. Patient ran embedded algorithm for 4 consecutive days (one month after (b) while wearing a PKG watch on the contralateral hand, and completing a motor diary. This was compared to watch and diary data collected on open loop chronic stimulation two weeks prior. Both objective (PKG wearable) and subjective (motor diary) measures indicate an increase in "on" time in comparison to open loop stimulation. aDBS = adaptive deep brain stimulation.

Author Manuscript Author Manuscript Author Manuscript Author Manuscript

Table 1.

Demographics of study subjects.

All clinical rating scores are obtained preoperatively within 90 days of DBS implantation.

Subject ID	Age at surgery and gender	Duration of motor signs (years)	MOCA	Levodopa equivalents (mg/day)*	MDS-UPDRS III off medication score	% change MDS-UPDRS when on	Time with dyskinesia**	Off tremor scores***
RCS01	54,M	7	26	1425	49	90%	4	left:2 right:0
RCS02	63,M	19	30	955	45	51%	1	left: 3 right: 4
RCS03****	28,F	12	27	1550	61	73%	2	left: 12 right: 9
RCS04	40,M	4	30	1314	41	65%	1	left: 6 right: 3
RCS05	58,M	12	27	2100	44	75%	2	left: 0 right: 0

* levodopa equivalents calculated with reference to: Tomlinson CL1, Stowe R, Patel S, Rick C, Gray R, Clarke CE. Mov Disord. 2010 Nov 15;25(15):2649–53. doi: 10.1002/mds.23429. Systematic review of levodopa dose equivalency reporting in Parkinson's disease.

** MDS-UPDRS part IV item 4.1

*** sum of all MDS-UPDRS-III tremor scores for each side, off medication (MDS-UPDRS-III items 16a through 17d)

**** positive for Parkin mutation

Abbreviations: MOCA - Montreal Cognitive Assessment

Nat Biotechnol. Author manuscript; available in PMC 2021 November 03.